

1 **MK2a inhibitor CMPD1 abrogates chikungunya virus infection by modulating actin
2 remodeling pathway.**

3 Prabhudutta Mamidi¹, Tapas Kumar Nayak^{3,2}, Abhishek Kumar^{4,1}, Sameer Kumar^{5,1}, Sanchari
4 Chatterjee^{1,6}, Saikat De¹, Ankita Datey¹, Eshna Laha¹, Amrita Ray¹, Subhasis Chattopadhyay^{2*},
5 Soma Chattopadhyay^{1*}

6 Running title: CMPD1 inhibits chikungunya virus infection.

7 ¹Institute of Life Sciences, Bhubaneswar, India

8 ²National Institute of Science Education and Research, Jatni, India.

9 ³Center for Translational Medicine, Lewis Katz School of Medicine,
10 Temple University, Philadelphia, PA 19140, United States of America

11 ⁴Department of Oral Biology, University of Florida College of Dentistry, Gainesville, Florida,
12 United States of America

13 ⁵Department of Microbiology and Immunology, Carver College of Medicine, University of Iowa,
14 Iowa city, United States of America.

15 ⁶Regional Centre for Biotechnology, Faridabad

16 ***Address of Corresponding author:**

17 Soma Chattopadhyay

18 Institute of Life Sciences,

19 Autonomous Institute of Dept of Biotechnology (Govt of India),

20 Nalco Square, Bhubaneswar-751023, India

21 Phone No: 0091 674 2304235; Fax No: 0091 674 2300728

22 Email: sochat.ils@gmail.com

23

24 Subhasis Chattopadhyay
25 School of Biological Sciences,
26 National Institute of Science Education & Research,
27 Bhubaneswar, HBNI, Jatni, Khurda,
28 Odisha, 752050, India.
29 Email: subho@niser.ac.in.

30

31

32

33

34 Key Words: Chikungunya, Alphavirus, MK2, MK3, CMPD1

35

36

37

38

39

40

41

42

43

44 **Abstract**

45 Chikungunya virus (CHIKV) epidemics around the world have created public health concern
46 with the unavailability of effective drugs and vaccines. This emphasizes the need for molecular
47 understanding of host-virus interactions for developing effective targeted antivirals. Microarray
48 analysis was carried out using CHIKV strain (Prototype and Indian) infected Vero cells and two
49 host isozymes, MK2 and MK3 were selected for further analysis. Gene silencing and drug
50 treatment were performed *in vitro* and *in vivo* to unravel the role of MK2/MK3 in CHIKV
51 infection. Gene silencing of MK2 and MK3 abrogated around 58% CHIKV progeny release from
52 the host cell and a MK2 activation (a) inhibitor (CMPD1) treatment demonstrated 68% inhibition
53 of viral infection suggesting a major role of MAPKAPKs during the late phase of CHIKV
54 infection *in vitro*. Further, it was observed that the inhibition in viral infection is primarily due to
55 the abrogation of lamellipodium formation through modulation of factors involved in the actin
56 cytoskeleton remodeling pathway that is responsible for releasing the virus from the infected
57 cells. Moreover, CHIKV-infected C57BL/6 mice demonstrated reduction in the viral copy
58 number, lessened disease score and better survivability after CMPD1 treatment. In addition,
59 reduction in expression of key pro-inflammatory mediators such as CXCL13, RAGE, FGF,
60 MMP9 and increase in HGF (a CHIKV infection recovery marker) was observed indicating the
61 effectiveness of this drug against CHIKV. Additionally, CMPD1 also inhibited HSV1 and SARS
62 CoV2-19 infection *in vitro*. Taken together it can be proposed that MK2 and MK3 are crucial
63 host factors for CHIKV infection and can be considered as key targets for developing effective
64 anti-CHIKV strategies in future.

65

66

67 **Author summary**

68 Chikungunya virus has been a dreaded disease from the first time it occurred in 1952 Tanzania.
69 Since then it has been affecting the different parts of the world at different time periods in large
70 scale. It is typically transmitted to humans by bites of *Aedes aegypti* and *Aedes albopictus*
71 mosquitoes. Although, studies have been undertaken to combat the disease still there are no
72 effective strategies like vaccines or antivirals against it. Therefore it is essential to understand the
73 virus and host interaction to overcome this hurdle. In this study two host factors MK2 and MK3
74 have been taken into consideration to see how they regulate the multiplication of the virus. The
75 *in vitro* experiments demonstrated that inhibition of MK2 and MK3 restricted viral infection
76 Further, it was observed that this is due to the blocking of lamellipodium formation by modifying
77 the factors involved in the actin cytoskeleton remodeling pathway that is responsible for
78 releasing the virus from the infected cells. Besides, decreased disease score as well as better
79 survivability was noticed in the *in vivo* experiments with mice. Therefore, MK2 and MK3 could
80 be considered as the key targets for controlling CHIKV infection.

81

82

83

84

85

86

87

88

89

90 **Introduction**

91 The Chikungunya virus (CHIKV) is an insect-borne virus belonging to the genus *Alphavirus* and
92 family *Togaviridae* and transmitted to humans by *Aedes* mosquitoes(1). Three CHIKV
93 genotypes, namely West African, East Central South African and Asian have been identified.
94 The incubation period ranges from two to five days following which symptoms such as fever (up
95 to 40°C), petechial or maculopapular rash of the trunk and arthralgia affecting multiple joints
96 develop(2-4).

97 CHIKV is a small (60-70nm diameter), spherical, enveloped, positive sense single-stranded RNA
98 (~12Kb) virus (5-7). Its genomic organization is 5'-cap-nsP1-nsP2-nsP3-nsP4-(junction region)-
99 C-E3-E2-6K-E1-3'(8). The non-structural proteins (nsP1-4) are primarily involved in virus
100 replication, while structural proteins C, E3, E2, 6K and E1 are responsible for packaging and
101 producing new virions.

102 In India, CHIKV infection has re-emerged with the outbreak of 2005–08 affecting approximately
103 1.3 million people in 13 different states (9). The clinical manifestations during these outbreaks
104 were found to be more severe leading to the speculation that either a more virulent or an
105 efficiently transmitted variant of this virus might have emerged (10).

106 CHIKV, among most other viruses across families, interacts with a number of cellular proteins
107 and consequently metabolic pathways to aid its survival in the host (11-17). Several facets of
108 CHIKV pertaining to strategies required for ecological success, replication, host interaction and
109 genetic evolution are yet to be fully explored and are constantly evolving. This spurs the need to
110 identify important host pathways that can be targeted for developing antiviral therapies against
111 the virus.

112 Alternatively, host factors involved in viral replication may also be targeted. Previous studies
113 have shown compounds targeting furin, protein kinases, and Hsp90, are inhibiting CHIKV
114 replication *in vitro* (18-20). However, further validation through *in vivo* experiments and pre-
115 clinical studies need to be performed prior to developing effective antivirals.
116 Our group has formerly reported an Indian outbreak strain IS, to exhibit a faster replication rate
117 than the CHIKV prototype strain, PS *in vitro* (21). The present study identifies host genes which
118 are modulated differentially during CHIKV infection in mammalian system and explores the
119 involvement of MAPK-activated protein kinases during virus infection using both *in vitro* and *in*
120 *vivo* conditions through inhibitor studies.

121 **Materials and Methods**

122 **Cells, Viruses, Antibodies, Inhibitors**

123 Vero cells (African green monkey kidney cells), CHIKV strains, prototype strain, PS (**Accession**
124 **no: AF369024.2**) and novel Indian ECSA strain, IS (**Accession no: EF210157.2**) and E2
125 Monoclonal antibody were gifted by Dr. M. M. Parida, DRDE, Gwalior, India. The HSV-1 virus
126 strain KOS with GenBank accession Number JQ673480.1 was kindly gifted by Dr. Roger
127 Everett, Glasgow University, Scotland. The HEK 293T cell line was gifted by Dr. Rupesh Dash,
128 Institute of Life Sciences, Bhubaneswar, India. **SARS details:** - The SARS-CoV-2 virus used in
129 this study was isolated from a clinically confirmed local COVID-19 patient (GISAID accession
130 ID- EPI_ISL_1196305). Virus from the 10th passage was used for experiments. Cells were
131 maintained in Dulbecco's Modified Eagle's medium (DMEM; PAN Biotech, Germany)
132 supplemented with 5% Fetal Bovine Serum (FBS; PAN Biotech), Gentamicin and Penicillin-
133 Streptomycin (Sigma, USA).The anti-nsP2 monoclonal antibody used in the experiments was
134 developed by us(22). Cofilin monoclonal antibody was purchased from Cell Signaling

135 Technologies (Cell Signaling Inc, USA). The pMK2 polyclonal antibody and MK3 monoclonal
136 antibody were purchased from Santacruz Biotechnology (USA). The p-Cofilin antibody and
137 GAPDH antibody were procured from Sigma Aldrich (USA) and Abgenex India Pvt. Ltd. (India)
138 respectively. Anti-mouse and anti-rabbit HRP-conjugated secondary antibodies were purchased
139 from Promega (USA). Alexa Fluor 488 and Alexa Fluor 594 antibodies were purchased from
140 Invitrogen (USA). The MK2a inhibitor, CMPD1 was purchased from Calbiochem (Germany).

141 **Virus infection**

142 The Vero cells were infected with PS/IS strains of CHIKV respectively according to the
143 experimental requirements as reported earlier (21). Thereafter, CHIKV infected cells were
144 incubated for 15-18hpi following which cells and supernatants were harvested from mock,
145 infected and drug treated samples for downstream processing. For HSV (Herpes Simplex Virus)
146 and SARS-CoV-2, Vero cells were infected with 0.1 MOI of virus and incubated for 22 hpi. The
147 supernatants were harvested at 22 hpi and subsequent downstream processing was carried out for
148 estimating the viral titers.

149 **RNA isolation and Microarray hybridization**

150 In the present study, the global gene expression analyses were carried out using Agilent Rhesus
151 GeneChip® ST arrays. Sample preparation was performed according to the manufacturer's
152 instruction (Agilent, USA). Briefly, RNA was extracted from mock and virus infected Vero cells
153 using the RNeasy mini kit (Qiagen, Germany). Next, RNA quality was assessed by Agilent
154 Bioanalyzer and cDNA was prepared using oligo dT primer incorporating a T7 promoter. The
155 amplified, biotinylated and fragmented sense-strand DNA targets were generated from the
156 extracted RNA and hybridized to the gene chip containing over 22,500 probe sets at 65°C for

157 17h at 10 rpm. After hybridization, the chips were stained, washed and scanned using a Gene
158 Chip Array scanner.(23)

159 **Microarray analysis**

160 Raw data sets were extracted from all text files after scanning the TIFF files. These raw data sets
161 were analyzed separately using the GeneSpring GX12.0 software (Agilent Technologies, USA)
162 followed by differential gene expression and cluster analysis. Differential gene expression
163 analyses were performed by using standard fold change cut off ≥ 2.0 and ≥ 10.0 against IS
164 (8hpi) vs Mock (8hpi), PS (8hpi) Vs Mock (8hpi), PS (18hpi) Vs Mock (18hpi), IS (8hpi) vs PS
165 (8hpi) and IS (8hpi) vs PS (18hpi). The hierarchical clustering was performed using the Genesis
166 software(24). Functional annotation of differentially expressed genes was carried out using the
167 PANTHER gene ontology analysis software (25).

168 **RNA extraction and qRT-PCR**

169 Equal volumes of serum isolated from all groups of mice samples were taken for viral RNA
170 isolation using the QiaAmpViral RNA isolation kit (Qiagen, USA) as per the manufacturer's
171 instructions. RT reaction was performed with 1 μ g RNA using the First Strand cDNA Synthesis
172 kit (Fermentas, USA) as per manufacturer's instructions. Equal volume of cDNA was used for
173 PCR amplification of E1 gene of CHIKV using specific primers (26). The nucleocapsid (NC)
174 gene of SARS-CoV-2 was amplified using forward primer- 5'-
175 GTAACACAAGCTTCGGCAG-3' and reverse primer- 5'-GTGTGACTTCCATGCCAATG-
176 3'. The viral copy number estimation from Ct values was estimated from the standard curve
177 generated for CHIKV E1 gene/ SARS-CoV-2 (NC) gene (data not shown).

178

179

180 **siRNA Transfection**

181 Monolayers of HEK 293T cells with 70% confluence (1×10^6 cells/well) in 6-well plates were
182 transfected separately or in combination with 60pmols of siRNA corresponding to MK2 mRNA
183 sequence [(5'-3')CCAUCACCGAGUUUAUGAAdTdT] and MK3 mRNA sequence [(5'-3')
184 GAGAACUGCAGAGAUAAUdTdT] or with siRNA negative control. Transfection was
185 performed using Lipofectamine-2000 (Invitrogen, USA) according to the manufacturer
186 instructions. In brief, HEK cells were transfected using Lipofectamine 2000 according to
187 different siRNA quantity in Opti-MEM medium (Thermo scientific, USA). The transfected cells
188 were infected with either CHIKV strains PS or IS with MOI 0.1 at 24 hours post transfection
189 (hpt). Eighteen hours post infection, the cells were harvested to measure the nsP2 and MK2/3
190 protein levels by Western blot analysis.

191 **SDS-PAGE and Western blot analysis**

192 Protein expression was examined by Western blot analysis as described earlier (21, 27). CHIKV
193 nsP2 and E2 proteins were detected with monoclonal antibodies (28) and re-probed with
194 GAPDH antibody to confirm the equal loading of samples. The pMK2, MK3, Cofilin and
195 pCofilin antibodies were used as recommended by the manufacturer. The Western blots were
196 scanned using the Quantity One Software (Bio Rad, USA).

197 **Plaque assay**

198 The CHIKV-infected cell culture supernatants were collected at 18 hpi and subjected to plaque
199 assay according to the procedure mentioned earlier (29).

200 **Immunofluorescence staining**

201 Immunofluorescence staining was carried out using the procedures described earlier (22). Vero
202 cells were grown on glass coverslips placed in 35mm dishes and infected with CHIKV (MOI

203 0.1) as described above. At 18 hpi, coverslips were stained with primary antibodies followed by
204 staining with secondary antibody (AF 594-conjugated anti-mouse antibody) for 45 mins. The
205 phalloidin staining was carried out using the Cytopainter F actin labeling kit as per
206 manufacturer's protocol (Abcam, UK). The coverslips were stained with DAPI for 90 sec and
207 mounted with 15-20 μ l Antifade (Invitrogen, USA) to reduce photo-bleaching. Fluorescence
208 microscopic images were acquired using the Leica TCS SP5 confocal microscope (Leica
209 Microsystems, Germany) with 63X objective and analyzed using the Leica Application Suite
210 Advanced Fluorescence (LASAF) V.1.8.1 software.

211 **Immunohistochemistry analysis:**

212 For histopathological examinations, tissue samples were dehydrated, embedded in paraffin wax,
213 and thereafter serial paraffin sections (5 μ m) were obtained (30). Briefly, the sections were
214 immersed in two consecutive xylene washes for de-paraffinization and were subsequently
215 hydrated with five consecutive ethanol washes in descending order of concentration: 100%, 90%,
216 70%, and deionized water. The paraffin sections were then stained with hematoxylin-eosin
217 (H&E), and histopathological changes were visualized using a light microscope (Zeiss Vert.A1,
218 Germany).

219 **Cellular cytotoxicity assay**

220 Cellular cytotoxicity assay was performed as described earlier (31). Vero cells were seeded onto
221 96-well plates at a density of 3000 cells/well, treated with different concentrations of CMPD1 for
222 24 hrs at 37°C with 5% CO₂. DMSO-treated samples served as control. After incubation, 10 μ l of
223 MTT reagent (Sigma Aldrich, USA) was added to the wells followed by incubation at 37°C for
224 3hrs and processed further. Absorbance of the suspension was measured at 570nm using ELISA

225 plate reader (BioRad, USA). Cellular cytotoxicity was determined in duplicates and each
226 experiment was repeated thrice independently.

227 **CMPD1 treatment**

228 Vero cells with 90% confluence were grown in 35mm or 60mm cell culture dishes (according to
229 the experimental requirements) and infected with PS or IS strains of CHIKV as described above
230 at MOI 0.1. After infection, cells were treated with either DMSO or different concentrations of
231 CMPD1 as per the protocol mentioned earlier (32). The cells were observed for detection of
232 cytopathic effect (CPE) under 10X objective of bright field microscope. Infected cells and
233 supernatants were then collected at 15-18hpi depending on the experiment.

234 **Time of addition experiment**

235 Vero cells were infected with CHIKV as described above and CMPD1 (50 μ M) was added at 1hr
236 interval upto 11hrs to the infected cells in different dishes. Thereafter, cell culture supernatants
237 of all the samples were harvested at 15hpi and plaque assay was carried out for estimating viral
238 titer.

239 **CHIKV infection in mice**

240 The mice related experiments were performed as per CPCSEA guidelines and were approved by
241 the IAEC committee. Around 10-14 days old male C57BL/6 mice (n=5) were injected
242 subcutaneously with 1×10^6 particles of IS in DMEM. At 3hpi, mice were fed with CMPD1 at a
243 concentration of 5mg/kg of body weight and continually fed at every 24hr-interval up to 3 days.
244 All mice were sacrificed on the fourth day; blood samples were harvested from mock, infected
245 and drug-treated samples and used for downstream processing. For survival curve analysis,
246 CHIKV-infected mice were fed with CMPD1 and observed every day, for CHIKV-induced
247 disease manifestations up to 8 days post infection (dpi). All infected mice were scored on a scale

248 of 0 to 6 based on CHIKV induced disease symptoms such as(0- No symptoms, 1- lethargic, 2-
249 ruffled fur, 3- restricted movement/limping, 4- one hind limb paralysis and 5 – both hind limb
250 paralysis 6- Morbid/dead).

251 **Proteome profiling**

252 In order to assess the levels of different cytokines in mock, CHIKV-infected and CHIKV-
253 infected+drug treated mice samples, proteome profiling was performed using the Mouse XL
254 cytokine array kit (R & D systems, USA) as per manufacturer's instructions. The array blots
255 were incubated with serum samples at 4°C overnight on a gel rocker, followed by incubation
256 with HRP-conjugated secondary antibody. Blots were developed using the chemiluminescent
257 HRP substrate and scanned by the Image Lab software (Bio-Rad, USA). The relative differences
258 in expression patterns of selected cytokines among the different groups of samples were assessed
259 using the GraphPadPrism8 software.

260 **Bioavailability Prediction:** - The bioavailability of CMPD1 was predicted through the SWISS
261 ADME tool available in the website (www.swissadme.ch). The SMILE structure of CMPD1 was
262 submitted to the tool for analysis and prediction.

263 **Statistical analysis**

264 Statistical analysis of the experimental data was performed by using the GraphPad Prism 8.0
265 Software and presented as mean \pm SD of three independent experiments. The One-way ANOVA
266 with Dunnet post-hoc test was used to compare the differences between the groups. In all the
267 tests, p value < 0.05 was considered to be statistically significant.

268

269

270 **Accession numbers**

271 The accession number for the submitted microarray experimental data to Array Express database
272 is **E-MTAB-6645**. The URL for the submitted microarray experimental data is as
273 follows: *http://www.ebi.ac.uk/arrayexpress/experiments/E-MTAB-6645*.

274 **Results**

275 **Differential host gene expressions for PS and IS strains of CHIKV in Vero cells.**

276 Earlier, it was observed that CPE developed by IS was more prominent at 8 hpi as compared to
277 PS which showed similar CPE around 18 hpi(21). To understand the host gene expression
278 profiles for the two CHIKV strains, Vero cells were harvested at 8 and 18 hpi for microarray
279 analysis. Microarray data revealed the differential expression of 20227 genes, of which 12221
280 genes were differentially expressed after applying fold change cut off ≥ 2.0 . Further, 684 genes
281 from the 12221 were differentially expressed with fold change ≥ 10.0 . The cluster analysis of
282 differentially expressed genes was carried out using the GENESPRING GX 12.0 software, as
283 shown in Fig 1A. Annotation of the total genes into different protein classes was carried out
284 using the Panther software. It was observed that majority of the genes belonged to the nucleic
285 acid binding molecules, signaling molecules, transcription factors among others, as represented
286 in Fig 1B. A pie-chart was constructed using the Panther software to annotate these genes into
287 different biological processes, and it was observed that majority of the modulated genes
288 belonged to the pathways involved in different cellular processes (Fig 1C). Moreover, 720 genes
289 were differently regulated by IS alone as depicted by the Venn diagram constructed through the
290 Gene Venn software in (Fig 1D and 1E). Out of these 720 genes, few selected genes were
291 functionally annotated into different host cellular pathways as shown in “S1 Table”. MK3 was

292 present among the 720 genes that were antagonically expressed in IS infected cells at 8 hpi in
293 comparison to PS (8 and 18 hpi). The importance of MK3 and its isozyme partner MK2 was thus,
294 deliberated during CHIKV infection in this study. Together, the data indicate that CHIKV
295 utilizes different host cell pathways for efficient replication inside the host cell and there are
296 differential host gene expression patterns for various strains of CHIKV.

297 **MK2 and MK3 gene silencing abrogates CHIKV progeny release without affecting viral**
298 **protein synthesis.**

299 To elucidate the importance of MK2 and MK3 in CHIKV infection, gene silencing through
300 siRNA approach was employed. Since the transfection efficiency of Vero cells is poor,
301 HEK293T cell line (Kidney epithelial cell line) was used for this experiment. HEK293T cells
302 were transfected with 60 pmol of MK2 and/or MK3 siRNAs and incubated for 24 hrs at 37°C.
303 Next, the siRNA transfected cells were infected with CHIKV [(PS/IS), MOI 0.1] and cells as
304 well as supernatants were harvested at 18 hpi for further analysis. No remarkable change in nsP2
305 expression was observed after genetic knock down of either MK2 or MK3. Surprisingly, the
306 expression of CHIKV-nsP2 was increased marginally when both MK2 and MK3 were silenced
307 together as compared to control as shown in Fig 2A and 2B (left and right panels respectively).
308 As the expression of nsP2 was increased after siRNA treatment, plaque assay was performed to
309 assess the effect of MK2 and/or MK3 down-regulation in viral progeny formation. Interestingly,
310 it was observed that the viral titers were reduced by 58% for PS strain and 53% for IS strain as
311 shown in Fig 2C and 2D. Therefore, it can be suggested that MK2 and MK3 altogether affects
312 CHIKV progeny release without affecting viral protein synthesis.

313 **CMPD1, an MK2a inhibitor abrogates CHIKV infection *in vitro*.**

314 The MAPK-activated protein kinases MAPKAPK3 (MK3) and MAPKAPK2 (MK2) are the
315 substrates of P38 MAPK that form a pair of structurally and functionally closely related
316 enzymes. Being highly homologous enzymes (around 70% at the amino acid sequence), their
317 substrate spectrums are indistinguishable(33). MK2 expression levels usually exceeds MK3 level
318 in cells, however, in absence of functional MK2, MK3 compensates.

319 To investigate the role of MK2 pathway in CHIKV infection, Vero cells were treated with a non-
320 ATP competitive MK2 inhibitor, CMPD1, which selectively inhibits P38-mediated MK2
321 activation (34). In order to determine the cytotoxicity of CMPD1, Vero cells were treated with
322 different concentrations of the drug (25, 50, 75 and 100 μ M) for 24 h and MTT assay was
323 performed. It was observed that 98%, 95% and 85% cells were viable with 25, 50 and 100 μ M
324 concentrations of the drug, respectively, as shown in Figure 3a. Next, dose kinetics assay was
325 performed to determine the anti-CHIKV efficacy of CMPD1. Therefore, Vero cells were infected
326 with two different strains of CHIKV with MOI 0.1 and treated with 25, 50 and 100 μ M
327 concentrations of CMPD1. The cell culture supernatants were harvested at 18 hpi and plaque
328 assay was carried out to estimate the virus titers. Around 90% decrease in virus titer was
329 observed with higher concentrations of CMPD1 in comparison to DMSO control for both the
330 strains (Fig 3B and 3C). Since, effect of CMPD1 was same for both the strains, IS strain (more
331 virulent of the two strains used in this study) was used for further experiments.

332 To estimate the IC₅₀ value of CMPD1, Vero cells were infected with CHIKV as mentioned
333 above and different concentrations of CMPD1 (10-100 μ M) were added to the cells post-
334 infection. The supernatants were harvested at 18 hpi and plaque assay was performed. The
335 plaque numbers were converted into log 10 of PFU/mL and plotted in the graph as shown in Fig
336 3D. The IC₅₀ of CMPD1 was found to be 33.97 μ M.

337 Next, to assess the possible mechanism of action of CMPD1 on CHIKV replication, time of
338 addition experiment was performed. Vero cells were infected with IS strain with MOI 0.1 and 50
339 μ M of CMPD1 was added at 1hr interval from 0–11 hpi. DMSO was used as a control. Next, the
340 CHIKV-infected and CMPD1 treated supernatants were harvested at 15 hpi and plaque assay
341 was performed as mentioned above to assess the release of infectious virus particles. As shown
342 in Fig 3E, it was observed that around 55% of the infectious virus particle release was abrogated
343 in the presence of 50 μ M of CMPD1, even after the addition of the drug at 11 hpi. This indicates
344 that CMPD1 inhibits later phase of CHIKV life cycle.

345 Lastly, to understand the role of CMPD1 in CHIKV packaging/release, Vero cells were infected,
346 drug-treated, and supernatants were collected at 18 hpi for estimating the extracellular viral titer
347 through plaque assay. For estimating the intracellular virus titer, cells were washed twice with
348 1X PBS and harvested. The pelleted cells were resuspended in fresh serum free medium and
349 freeze-thawed thrice to release virus particles trapped inside the cells. Then the plaque assay was
350 performed using the supernatant to estimate the intracellular virus titer. Similar to the previous
351 experiment, the extracellular virus titer was around 70% less in CMPD1 treated samples in
352 comparison to control but the intracellular virus titer was around 60% more for CMPD1 treated
353 samples as shown in Fig 3F and 3G. This suggests that CMPD1 did not inhibit the
354 formation/packaging of newly synthesized host particles inside the host cell; however, it affects
355 the release of CHIKV viral progeny from the host cell.

356

357 **CMPD1 blocks the actin polymerization process modulated by CHIKV for its progeny**
358 **release.**

359 It is well known that both the isozymes, MK2 and MK3 are exclusively phosphorylated by P38
360 MAPK and both have similar substrates (35). It is also known that LIM kinase 1 (LIMK1), a
361 downstream substrate of MK2 induces actin polymerization by phosphorylating and inactivating
362 cofilin, an actin-depolymerizing factor (36, 37). Therefore, to understand the effect of CMPD1 in
363 viral infection and on downstream substrates of MK2, the cells were infected with IS at MOI 0.1
364 and treated with 50 μ M CMPD1. Infected cells were observed for the development of CPE at 18
365 hpi and clear reduction in CPE was observed after CMPD1 treatment (Fig 4A). The cells were
366 harvested at 18 hpi and cell lysates were processed for Western blot analysis. It was noticed that
367 the levels of pMK2 and MK3 were downregulated after drug treatment with no change in
368 CHIKV nsP2 expression as shown in Fig 4B and 4C. Similarly, the expression of Cofilin and p-
369 Cofilin was decreased in the presence of CMPD1. The expression of pMK3 could not be tested
370 due to unavailability of a commercial antibody. Altogether, the data suggest that MK2
371 phosphorylation plays an important role in viral progeny release by modulating the actin
372 polymerization process.

373 In order to confirm the involvement of actin fibers in CHIKV progeny release, Vero cells were
374 virus infected and drug treated as mentioned above and cells were fixed at 18 hpi. Thereafter,
375 phalloidin staining was carried out to stain actin fibers in cells as it has been reported that
376 fluorescent dye-labeled phalloidin stains only the actin fibers, but not the monomers (38).
377 Phalloidin staining was found to be more prominent in infected cells without CMPD1 treatment
378 and was more diffusely stained in CMPD1 treated infected cells. Furthermore, the expression
379 pattern of CHIKV E2 protein was unchanged in both the samples as shown in Fig 4D. Taken
380 together, the results depict that CHIKV utilizes the actin polymerization process for its progeny

381 release through activation of MK2/MK3; however CMPD1 abrogates the whole process by
382 inhibiting MK2/3 activation.

383 **CMPD1 inhibits CHIKV infection *in vivo*.**

384 In order to assess the bio-availability of a drug/inhibitor, computer models have been used as a
385 valid alternative to experimental procedures for prediction of ADME (Absorption, Distribution,
386 Metabolism and Excretion) parameters (39). The SwissADME Web tool (www.swissadme.ch) is
387 one such tool which enables the computation of key physicochemical, pharmacokinetic, drug-
388 like and related parameters for one or multiple molecules (40). Hence, the bioavailability of
389 CMPD1 was predicted through the SwissADME tool and it was found that CMPD1 has high GI
390 (Gastro Intestinal) absorption with a bioavailability score of 0.55 as shown in “S2 Table”.

391 In order to assess the antiviral effect of CMPD1 on CHIKV infection *in vivo*, 10-14 days old
392 male C57BL/6 mice (n=5 per group) were infected with the IS strain and serum as well as tissue
393 samples were harvested as per the protocol mentioned above. Viral RNA was isolated from the
394 pooled serum samples (from respective group) and RT-PCR was carried out to amplify E1 gene
395 of CHIKV. It was observed that the viral copy number was reduced remarkably (90%) in
396 CMPD1 treated CHIKV infected mice in comparison to control (Fig 5A). Next, to compare the
397 extent of tissue inflammation due to CHIKV infection in presence of drug, muscle tissue sections
398 (from the site of injection) of the sacrificed mice at 4dpi were stained using Haematoxylene and
399 Eosin and it was found that the infiltration of immune cells were less in CMPD1 treated tissue in
400 comparison to control as shown in Fig 5B. Furthermore, to determine the relative levels of
401 different cytokines/chemokines in CMPD1 treated mice, proteome profiling was carried out with
402 the pooled serum samples as described above. It was noticed that the expressions of few selective
403 inflammatory cytokines/chemokines, like CXCL13, RAGE, FGF and MMP9 were significantly

404 reduced in CMPD1 treated mice sera, as shown in Fig 5C and 5D. Interestingly, HGF was
405 upregulated in CMPD1 treated mice. To assess the protective action of CMPD1, survival curve
406 analysis was performed. For that, CHIKV infected mice (5 per group) were fed with CMPD1
407 (5mg/kg) orally at 3hrs post CHIKV infection and then for 3 consecutive days at an interval of
408 24 hrs. The disease scoring was performed based on the symptoms described in the methods
409 section and shown in “S3 Table”. Moreover, from the survival curve analysis as shown in Figure
410 5e, there was 100% mortality of the untreated CHIKV infected mice after 8 days post infection.
411 In contrast, no mortality was observed for the CMPD1 treated CHIKV infected mice even after 8
412 days post infection. The data suggests that CMPD1 shows anti-CHIKV activity *in vivo*.

413 **CMPD1 modulates HSV and SARS CoV2 infection *in vitro*.**

414 In order to assess the efficacy of CMPD1 against other viruses like HSV-1 and SARS-CoV-2,
415 Vero cells were infected with 0.1 MOI of HSV and SARS-CoV-2 separately and treated with
416 different concentrations of CMPD1 post infection. The cells were incubated for 22 hpi and
417 distinct morphological changes were visible under microscope between infected and drug treated
418 cells as shown in Fig 6A and 6C. In case of HSV-1, the supernatants of infected and drug treated
419 cells were harvested at 22 hpi and plaque assay was carried out to estimate the viral titers. It was
420 observed that there was around 45% inhibition with 25 μ M and 90% inhibition in viral titers with
421 50 μ M of CMPD1 as shown in Fig 6B. However, in case of SARS-CoV-2, viral RNA was
422 extracted from the supernatants at the same time point and cDNA synthesis was carried out.
423 Then, the Nucleocapsid (NC) gene of SARS-CoV-2 was amplified by qRT-PCR using the gene
424 specific primers [Forward: GTAACACAAAGCTTCGGCAG and Reverse:-
425 GTGTGACTTCCATGCCAATG]. The copy number of the virus was calculated from the Ct
426 value using the standard curve. It was observed that there was around 60% reduction with 50 μ M

427 of CMPD1 and 88% reduction with 75 μ M of CMPD1 as shown in Fig 6 D. The results indicate
428 that CMPD1 is effective against other viruses like HSV-1 and SARS CoV2 *in vitro*.

429 **Discussion**

430 CHIKV is now considered as a major public health concern. Due to lack of therapeutics and
431 vaccine, a number of studies have been initiated to understand the function of viral proteins and
432 the mechanisms of virus-mediated manipulation of host machineries for successful replication
433 (41-43). The current investigation, aims to determine how host proteins are modulated during
434 CHIKV infection in mammalian cell lines. In this regard, microarray analysis was carried out for
435 mock and CHIKV-infected Vero cells and two genes MK2 and MK3 belonging to P38MAPK
436 pathway were selected for further analysis.

437 Gene silencing of MK2 and MK3 abrogated around 58% CHIKV progeny release from the host
438 cell and a MK2 activation inhibitor (CMPD1) treatment demonstrated 68% inhibition of viral
439 infection suggesting a major role of MAPKAPKs during late CHIKV infection *in vitro*. Further,
440 it was observed that the inhibition in viral infection is primarily due to the abrogation of
441 lamellipodium formation through modulation of factors involved in the actin cytoskeleton
442 remodeling pathway which is essential for virus release. Moreover, CHIKV-infected C57BL/6
443 mice demonstrated reduction in the viral copy number, lessened disease score and better
444 survivability after CMPD1 treatment. In addition, reduction in expression of key pro-
445 inflammatory mediators such as CXCL13, RAGE, FGF, MMP9 and increase in HGF (a CHIKV
446 infection recovery marker) was observed indicating the effectiveness of this drug against
447 CHIKV. Additionally, CMPD1 also inhibited the HSV1 and SARS CoV2-19 infection *in vitro*.
448 The roles of MK2 and MK3 have been implicated in few other viruses like Dengue (DENV),
449 Murine Cytomegalovirus (MCMV), Kaposi's Sarcoma Herpes Virus (KSHV), Rous Sarcoma

450 Virus (RSV), Influenza A and Human Immunodeficiency Virus (HIV). In DENV, it was found
451 that SB203580 (a P38MAPK inhibitor) treatment significantly reduced the phosphorylation of
452 MAPKAPK2 and other substrates such as HSP27 and ATF2 which reduced DENV-induced liver
453 injury in mice (44). In the case of MCMV, MK2 was reported to regulate cytokine responses
454 towards acute infection, via IFNARI-mediated pathways and prevents formation of intrahepatic
455 myeloid aggregates during infection (45). For KSHV, it was observed that the viral Kaposin B
456 (KapB) protein binds and activates MK2, thereby selectively blocking decay of AU-rich mRNAs
457 (ARE-mRNAs) that encode pro-inflammatory cytokines and angiogenic factors during latent
458 KSHV infections (46). Furthermore, it was noticed that during RSV infection, pP38 is
459 sequestered inside cytoplasmic inclusion bodies (IBs) resulting in substantial reduction in
460 accumulation of MK2 and suppressing cellular responses to virus infection. Additionally,
461 CMPD1 treatment reduced viral protein expression suggesting the importance of pMK2 in RSV
462 protein translation (32). In case of Influenza A, it was observed that MK2 and MK3 are activated
463 on virus infection enabling the virus to escape the antiviral action of PKR (47). Recently, it has
464 been shown that CCR5-tropic HIV induces significant reprogramming of host CD4+ T cell
465 protein production pathways and induces MK2 expression upon viral binding to the cell surface
466 that are critical for HIV replication in host cells (48). However, reports pertaining to the
467 involvement of MK2 and MK3 in alphavirus infection are not available. Hence, this
468 investigation is one of the first to highlight the importance of MK2 and MK3 in CHIKV.

469 According to the results, it can be suggested that both MK2 and MK3 play important roles in
470 CHIKV progeny release during CHIKV infection. After CHIKV infection, MK2 is
471 phosphorylated which in turn phosphorylates LIMK1.(37) The LIMK1 then inactivates Cofilin
472 by phosphorylating it (36) This results in accumulation of more p-Cofilin inside the cell than

473 active Cofilin. As a result, Cofilin is unable to cleave the actin filaments into monomers. This
474 leads to polymerization of actin filaments and subsequent lamellipodia formation which results
475 in effective CHIKV progeny release, as shown in Fig 7A. However, CMPD1 treatment abrogates
476 MK2/3 phosphorylation as a result of which LIMK is not able to inactivate Cofilin. Active
477 Cofilin then cleaves actin polymers to monomers, thereby preventing lamellipodium formation
478 and subsequent viral progeny release as shown in Fig 7B. Furthermore, *in vivo* studies
479 demonstrate that CMPD1 treated mice do not develop complications post CHIKV infection. This
480 can be speculated by the reduction in the expressions of certain virus induced inflammatory
481 chemokines and cytokines like CXCL13, RAGE and FGF in CMPD1 treated mice sera. The
482 involvements of these chemokines and cytokines have been reported for other virus infections
483 before (49-51). Additionally, the expression of MMP9, a host factor involved in the degradation
484 of extracellular matrix thereby promoting viral spread to neighbouring tissues (51) was also
485 reduced in drug-treated samples indicating abrogation of viral transmission during CMPD1
486 treatment. In contrast, the expression of HGF (a known marker for CHIKV recovery during acute
487 infection) (52) was upregulated during CMPD1 treatment thereby showing the effectiveness of
488 CMPD1 against CHIKV in a mouse model. Nevertheless, it would be interesting to understand
489 the detailed mechanism and role of these factors during CHIKV infection in future.

490 Thus, the current study highlights the importance of MK2 and MK3 (substrates of the p38MAPK
491 pathway) as novel host factors involved during CHIKV infection. It also demonstrated CMPD1
492 as a novel inhibitor of CHIKV infection; hence, CMPD1 can be pursued as a potential lead for
493 developing anti-CHIKV molecule to regulate disease manifestations.

494

495

496 **Figure legends**

497 **Fig 1:- Differential host gene expressions for PS and IS strains of CHIKV in Vero cells. (A)**

498 Hierarchical clustering showing the overall expression patterns of the modulated host genes by
499 PS/IS strains of CHIKV during infection in mammalian cells. **(B)** Pie-chart depicting the
500 distribution of the host genes in CHIKV-infected samples into different protein classes. **(C)** Pie-
501 chart depicting the distribution of the modulated host genes into different cellular processes. **(D**
502 **and E)** Venn diagram showing both commonly and differentially regulated host genes in
503 CHIKV (PS/IS) infected Vero cells.

504 **Fig 2:- MK2 and MK3 gene silencing abrogates CHIKV progeny release without affecting**

505 **viral protein synthesis. (A and B)** After 24 hrs post transfection with 60 pmol of MK2/3 siRNA
506 (either separately/in combination), cells were super-infected (PS/IS MOI 0.1) and harvested at 18
507 hpi. Western blot showing the expression levels of different proteins (Left panel). Bar diagrams
508 showing relative band intensities of different proteins (Right panel). GAPDH was used as
509 control. **(C and D)** Bar diagram showing the viral titres after siRNA treatment for PS and IS
510 strains, (n=3; $p<0.05$).

511 **Fig 3:- CMPD1, an MK2a inhibitor abrogates CHIKV infection *in vitro*. (A)** Vero cells were

512 treated with different concentrations of CMPD1 (25, 50, 75 and 100 μ M) for 24 h and MTT
513 assay was performed. **(B and C)** Vero cells infected with CHIKV PS/IS at MOI 0.1 and drug
514 treated. Bar graph showing the viral titers in the presence of CMPD1 (25, 50 and 100 μ M). **(D)**
515 Dose response curve showing the IC50 of CMPD1 against CHIKV. **(E)** Bar graph showing the
516 viral titers estimated through plaque assay from the supernatants obtained from the time of
517 addition experiment for CMPD1(50 μ M) post CHIKV infection. **(F and G)** Bar graph showing
518 intracellular and extracellular virus titers for samples harvested at 18hpi. DMSO was used as

519 control. All the graphs depict the values of mean \pm SD ($*p < 0.05$) of three independent
520 experiments.

521 **Fig 4:-CMPD1 blocks the actin polymerization process modulated by CHIKV for its**
522 **progeny release.** Vero cells were infected with the IS strain (0.1 MOI), 50 μ M of CMPD1 was
523 added to the cells and incubated for 18 hpi. **(A)** Bright field images (20X magnification) showing
524 the cytopathic effect after CHIKV infection with or without CMPD1 treatment (50 μ M). **(B)**
525 Western blot analysis showing the expressions of nsP2, pMK2, MK3, Cofilin and p-Cofilin
526 proteins. GAPDH served as the loading control. **(C)** Bar graphs showing the relative fold change
527 in viral and host proteins expression with respect to DMSO control. **(D)** Confocal microscopy
528 images showing the levels of E2 and phalloidin during CHIKV infection.

529 **Fig 5:- CMPD1 inhibits CHIKV infection in mice.** **(A)** Bar graph showing the viral copy
530 numbers in CHIKV infected and CMPD1 treated mouse serum samples. **(B)** H and E staining of
531 mouse tissue samples with CHIKV infection and in presence/absence of CMPD1. **(C)** Array blot
532 showing the expression of different cytokines after CHIKV infection in presence and absence of
533 CMPD1. **(D)** Bar graph showing the relative band intensities of selected cytokines in mock,
534 CHIKV infected and CMPD1 treated samples. **(E)** Survival curve showing the effect of CMPD1
535 in CHIKV infected mice

536 **Fig 6:- CMPD1 modulates HSV-1 and SARS-CoV-2 infection *in vitro*.** Vero cells were
537 infected with HSV-1 and SARS-CoV-2 (MOI 0.1) and treated with different concentrations of
538 CMPD1. **(A and C)** Bright field images showing CPE in presence of CMPD1 for HSV-1 and
539 SARS-CoV-2 infection. Black arrows indicate infected cells for HSV-1 and glowing cells
540 represent SARS-CoV-2 infected cells. **(B and D)** Bar graph showing viral titer/copy number in
541 presence of CMPD1 for HSV-1 and SARS-CoV-2 infection respectively.

542 **Fig 7:-Proposed model for CHIKV infection.** (A) During CHIKV infection, MK2/3 gets
543 phosphorylated by P38 MAPK thereby exposing the Nuclear Export Signal (NES) of MK2. The
544 phosphorylated forms of MK2/MK3 translocate to the cytoplasm and help in inactivating Cofilin
545 through phosphorylation via LIMK-1 thereby promoting actin polymerization and lamellipodium
546 formation. (B) Addition of CMPD1 blocks the phosphorylation of MK2, thereby blocking
547 Cofilin phosphorylation and eventually inhibiting lamellipodium formation and CHIKV progeny
548 release.

549 **Supplementary information**

550 S1 Table: - Differently modulated host genes for DRDE-06 classified into different metabolic
551 pathways.

552 S2 Table: - Bioavailability prediction of CMPD1 through SWISSADME web tool.

553 S3 Table: - Disease scoring of CHIKV infected and drug treated mice

554 **Authors Contribution:-**

555 SoC, SuC and PM conceived the idea and designed the experiments; PM, TKN, AK, SK, SC,
556 AD, SD and SM performed wet lab experiments; SoC and SuC contributed reagents; SoC, SuC
557 and PM analyzed and interpreted the data; SoC, PM , TKN, EL, AR and SuC wrote the
558 manuscript. All authors read and approved the final version of this manuscript.

559 **Acknowledgement:-**

560 We are thankful to Dr. M.M. Parida, DRDE, Gwalior, India for kindly providing IS and PS
561 strains of CHIKV and Vero cell line. We like to acknowledge Dr. Roger Everett, Glasgow
562 University, Scotland for providing the KOS strain of HSV-1. We are also grateful to Dr. Rupesh
563 Dash of ILS, Bhubaneswar, India for providing the HEK293T cell line.

564

565 **Funding:-**

566 This study has been funded by the Department of Science and Technology (DST-SERB), New
567 Delhi, India, vide grant no EMR/2016/000854. It was also supported by Institute of life sciences,
568 Bhubaneswar, under Department of Biotechnology and National Institute of Science Education
569 and Research (NISER), Bhubaneswar, under Department of Atomic Energy (DAE), Government
570 of India. We wish to acknowledge the University Grant Commission (UGC), New Delhi, India
571 for the fellowship to PM during this study.

572 **Transparency Declarations:-**

573 Nothing to declare.

574

575 **References:-**

- 576 1. Singh SK, Unni SK. Chikungunya virus: host pathogen interaction. *Reviews in medical virology*. 2011;21(2):78-88.
- 577 2. Jain M, Rai S, Chakravarti A. Chikungunya: a review. *Tropical doctor*. 2008;38(2):70-2.
- 578 3. Enserink M. Infectious diseases. Chikungunya: no longer a third world disease. *Science*. 2007;318(5858):1860-1.
- 579 4. Robinson MC. An epidemic of virus disease in Southern Province, Tanganyika Territory, in 1952-53. I. Clinical features. *Transactions of the Royal Society of Tropical Medicine and Hygiene*. 1955;49(1):28-32.
- 580 5. Higashi N, Matsumoto A, Tabata K, Nagatomo Y. Electron microscope study of development of Chikungunya virus in green monkey kidney stable (VERO) cells. *Virology*. 1967;33(1):55-69.
- 581 6. Powers AM, Brault AC, Tesh RB, Weaver SC. Re-emergence of Chikungunya and O'nyong-nyong viruses: evidence for distinct geographical lineages and distant evolutionary relationships. *The Journal of general virology*. 2000;81(Pt 2):471-9.
- 582 7. Strauss JH, Strauss EG. The alphaviruses: gene expression, replication, and evolution. *Microbiological reviews*. 1994;58(3):491-562.
- 583 8. Solignat M, Gay B, Higgs S, Briant L, Devaux C. Replication cycle of chikungunya: a re-emerging arbovirus. *Virology*. 2009;393(2):183-97.
- 584 9. Arankalle VA, Shrivastava S, Cherian S, Gunjikar RS, Walimbe AM, Jadhav SM, et al. Genetic divergence of Chikungunya viruses in India (1963-2006) with special reference to the 2005-2006 explosive epidemic. *The Journal of general virology*. 2007;88(Pt 7):1967-76.

596 10. Santhosh SR, Dash PK, Parida MM, Khan M, Tiwari M, Lakshmana Rao PV. Comparative full
597 genome analysis revealed E1: A226V shift in 2007 Indian Chikungunya virus isolates. *Virus research*.
598 2008;135(1):36-41.

599 11. Ludwig S, Pleschka S, Planz O, Wolff T. Ringing the alarm bells: signalling and apoptosis in
600 influenza virus infected cells. *Cellular microbiology*. 2006;8(3):375-86.

601 12. Rana J, Gulati S, Rajasekharan S, Gupta A, Chaudhary V, Gupta S. Identification of potential
602 molecular associations between chikungunya virus non-structural protein 2 and human host proteins.
603 *Acta virologica*. 2017;61(1):39-47.

604 13. Kim DY, Reynaud JM, Rasalouskaya A, Akhrymuk I, Mobley JA, Frolov I, et al. New World and Old
605 World Alphaviruses Have Evolved to Exploit Different Components of Stress Granules, FXR and G3BP
606 Proteins, for Assembly of Viral Replication Complexes. *PLoS pathogens*. 2016;12(8):e1005810.

607 14. Tossavainen H, Aitio O, Hellman M, Saksela K, Permi P. Structural Basis of the High Affinity
608 Interaction between the Alphavirus Nonstructural Protein-3 (nsP3) and the SH3 Domain of Amphiphysin-
609 2. *The Journal of biological chemistry*. 2016;291(31):16307-17.

610 15. Ashbrook AW, Lentscher AJ, Zamora PF, Silva LA, May NA, Bauer JA, et al. Antagonism of the
611 Sodium-Potassium ATPase Impairs Chikungunya Virus Infection. *mBio*. 2016;7(3).

612 16. Reid SP, Tritsch SR, Kota K, Chiang CY, Dong L, Kenny T, et al. Sphingosine kinase 2 is a
613 chikungunya virus host factor co-localized with the viral replication complex. *Emerging microbes &*
614 *infections*. 2015;4(10):e61.

615 17. Ooi YS, Dube M, Kielian M. BST2/tetherin inhibition of alphavirus exit. *Viruses*. 2015;7(4):2147-
616 67.

617 18. Ozden S, Lucas-Hourani M, Ceccaldi PE, Basak A, Valentine M, Benjannet S, et al. Inhibition of
618 Chikungunya virus infection in cultured human muscle cells by furin inhibitors: impairment of the
619 maturation of the E2 surface glycoprotein. *The Journal of biological chemistry*. 2008;283(32):21899-908.

620 19. Cruz DJ, Bonotto RM, Gomes RG, da Silva CT, Taniguchi JB, No JH, et al. Identification of novel
621 compounds inhibiting chikungunya virus-induced cell death by high throughput screening of a kinase
622 inhibitor library. *PLoS neglected tropical diseases*. 2013;7(10):e2471.

623 20. Rathore AP, Haystead T, Das PK, Merits A, Ng ML, Vasudevan SG. Chikungunya virus nsP3 & nsP4
624 interacts with HSP-90 to promote virus replication: HSP-90 inhibitors reduce CHIKV infection and
625 inflammation in vivo. *Antiviral research*. 2014;103:7-16.

626 21. Kumar A, Mamidi P, Das I, Nayak TK, Kumar S, Chhatai J, et al. A novel 2006 Indian outbreak
627 strain of Chikungunya virus exhibits different pattern of infection as compared to prototype strain. *PloS*
628 *one*. 2014;9(1):e85714.

629 22. Chattopadhyay S, Kumar A, Mamidi P, Nayak TK, Das I, Chhatai J, et al. Development and
630 characterization of monoclonal antibody against non-structural protein-2 of Chikungunya virus and its
631 application. *Journal of virological methods*. 2014;199:86-94.

632 23. Braicu C, Cojocneanu-Petric R, Jurj A, Gulei D, Tarantu I, Gras AM, et al. Microarray based gene
633 expression analysis of Sus Scrofa duodenum exposed to zearalenone: significance to human health. *BMC*
634 *genomics*. 2016;17:646.

635 24. Eisen MB, Spellman PT, Brown PO, Botstein D. Cluster analysis and display of genome-wide
636 expression patterns. *Proceedings of the National Academy of Sciences of the United States of America*.
637 1998;95(25):14863-8.

638 25. Mi H, Poudel S, Muruganujan A, Casagrande JT, Thomas PD. PANTHER version 10: expanded
639 protein families and functions, and analysis tools. *Nucleic acids research*. 2016;44(D1):D336-42.

640 26. Saswat T, Kumar A, Kumar S, Mamidi P, Muduli S, Debata NK, et al. High rates of co-infection of
641 Dengue and Chikungunya virus in Odisha and Maharashtra, India during 2013. *Infection, genetics and*
642 *evolution : journal of molecular epidemiology and evolutionary genetics in infectious diseases*.
643 2015;35:134-41.

644 27. Nayak TK, Mamidi P, Kumar A, Singh LP, Sahoo SS, Chattopadhyay S, et al. Regulation of Viral
645 Replication, Apoptosis and Pro-Inflammatory Responses by 17-AAG during Chikungunya Virus Infection
646 in Macrophages. *Viruses*. 2017;9(1).

647 28. Mishra P, Kumar A, Mamidi P, Kumar S, Basantray I, Saswat T, et al. Inhibition of Chikungunya
648 Virus Replication by 1-[(2-Methylbenzimidazol-1-yl) Methyl]-2-Oxo-Indolin-3-ylidene] Amino]
649 Thiourea(MBZM-N-IBT). *Scientific reports*. 2016;6:20122.

650 29. Chattopadhyay S, Weller SK. DNA binding activity of the herpes simplex virus type 1 origin
651 binding protein, UL9, can be modulated by sequences in the N terminus: correlation between
652 transdominance and DNA binding. *Journal of virology*. 2006;80(9):4491-500.

653 30. Priya R, Patro IK, Parida MM. TLR3 mediated innate immune response in mice brain following
654 infection with Chikungunya virus. *Virus research*. 2014;189:194-205.

655 31. Das I, Basantray I, Mamidi P, Nayak TK, B MP, Chattopadhyay S, et al. Heat shock protein 90
656 positively regulates Chikungunya virus replication by stabilizing viral non-structural protein nsP2 during
657 infection. *PloS one*. 2014;9(6):e100531.

658 32. Fricke J, Koo LY, Brown CR, Collins PL. p38 and OGT sequestration into viral inclusion bodies in
659 cells infected with human respiratory syncytial virus suppresses MK2 activities and stress granule
660 assembly. *Journal of virology*. 2013;87(3):1333-47.

661 33. Gaestel M. MAPKAP kinases - MKs - two's company, three's a crowd. *Nature reviews Molecular
662 cell biology*. 2006;7(2):120-30.

663 34. Davidson W, Frego L, Peet GW, Kroe RR, Labadia ME, Lukas SM, et al. Discovery and
664 characterization of a substrate selective p38alpha inhibitor. *Biochemistry*. 2004;43(37):11658-71.

665 35. Gaestel M. What goes up must come down: molecular basis of MAPKAP kinase 2/3-dependent
666 regulation of the inflammatory response and its inhibition. *Biological chemistry*. 2013;394(10):1301-15.

667 36. Yang N, Higuchi O, Ohashi K, Nagata K, Wada A, Kangawa K, et al. Cofilin phosphorylation by
668 LIM-kinase 1 and its role in Rac-mediated actin reorganization. *Nature*. 1998;393(6687):809-12.

669 37. Kobayashi M, Nishita M, Mishima T, Ohashi K, Mizuno K. MAPKAPK-2-mediated LIM-kinase
670 activation is critical for VEGF-induced actin remodeling and cell migration. *The EMBO journal*.
671 2006;25(4):713-26.

672 38. Neufeld DA, Hosman S, Yescas T, Mohammad K, Day F, Said S. Actin fiber patterns detected by
673 Alexafluor 488 phalloidin suggest similar cell migration in regenerating and nonregenerating rodent
674 toes. *The anatomical record Part A, Discoveries in molecular, cellular, and evolutionary biology*.
675 2004;278(1):450-3.

676 39. Dahlin JL, Inglese J, Walters MA. Mitigating risk in academic preclinical drug discovery. *Nature
677 reviews Drug discovery*. 2015;14(4):279-94.

678 40. Daina A, Michielin O, Zoete V. SwissADME: a free web tool to evaluate pharmacokinetics, drug-
679 likeness and medicinal chemistry friendliness of small molecules. *Scientific reports*. 2017;7:42717.

680 41. Abere B, Wikan N, Ubol S, Auewarakul P, Paemanee A, Kittisenachai S, et al. Proteomic analysis
681 of chikungunya virus infected microglial cells. *PloS one*. 2012;7(4):e34800.

682 42. Dhanwani R, Khan M, Lomash V, Rao PV, Ly H, Parida M. Characterization of chikungunya virus
683 induced host response in a mouse model of viral myositis. *PloS one*. 2014;9(3):e92813.

684 43. Thio CL, Yusof R, Abdul-Rahman PS, Karsani SA. Differential proteome analysis of chikungunya
685 virus infection on host cells. *PloS one*. 2013;8(4):e61444.

686 44. Sreekanth GP, Chuncharunee A, Sirimontaporn A, Panaampon J, Noisakran S, Yenchitsomanus
687 PT, et al. SB203580 Modulates p38 MAPK Signaling and Dengue Virus-Induced Liver Injury by Reducing
688 MAPKAPK2, HSP27, and ATF2 Phosphorylation. *PloS one*. 2016;11(2):e0149486.

689 45. Ehling C, Trilling M, Tiedje C, Le-Trilling VTK, Albrecht U, Kluge S, et al. MAPKAP kinase 2
690 regulates IL-10 expression and prevents formation of intrahepatic myeloid cell aggregates during
691 cytomegalovirus infections. *Journal of hepatology*. 2016;64(2):380-9.

692 46. Corcoran JA, Johnston BP, McCormick C. Viral activation of MK2-hsp27-p115RhoGEF-RhoA
693 signaling axis causes cytoskeletal rearrangements, p-body disruption and ARE-mRNA stabilization. PLoS
694 pathogens. 2015;11(1):e1004597.

695 47. Luig C, Kother K, Dudek SE, Gaestel M, Hiscott J, Wixler V, et al. MAP kinase-activated protein
696 kinases 2 and 3 are required for influenza A virus propagation and act via inhibition of PKR. FASEB
697 journal : official publication of the Federation of American Societies for Experimental Biology.
698 2010;24(10):4068-77.

699 48. Wiredja DD, Tabler CO, Schlatzer DM, Li M, Chance MR, Tilton JC. Global phosphoproteomics of
700 CCR5-tropic HIV-1 signaling reveals reprogramming of cellular protein production pathways and
701 identifies p70-S6K1 and MK2 as HIV-responsive kinases required for optimal infection of CD4+ T cells.
702 Retrovirology. 2018;15(1):44.

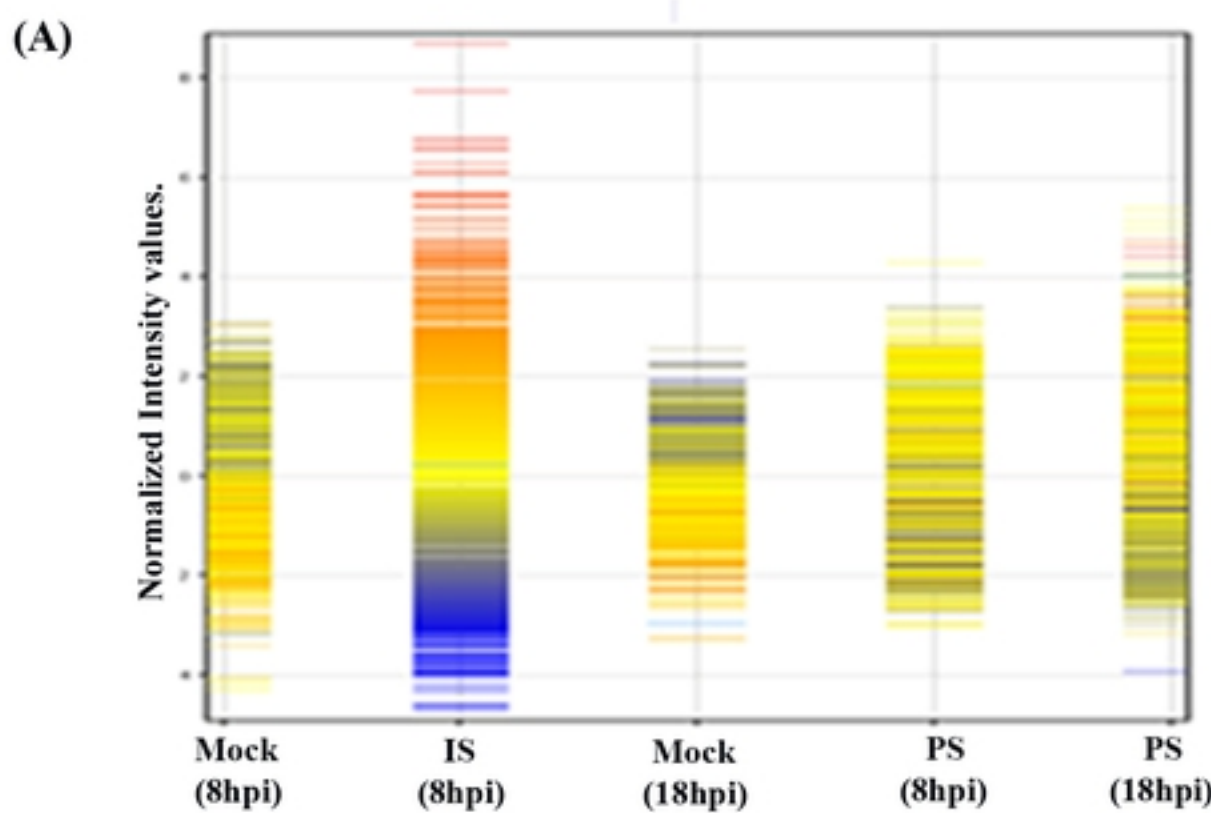
703 49. Rainey-Barger EK, Rumble JM, Lalor SJ, Esen N, Segal BM, Irani DN. The lymphoid chemokine,
704 CXCL13, is dispensable for the initial recruitment of B cells to the acutely inflamed central nervous
705 system. Brain, behavior, and immunity. 2011;25(5):922-31.

706 50. Mosquera JA. [Role of the receptor for advanced glycation end products (RAGE) in
707 inflammation]. Investigacion clinica. 2010;51(2):257-68.

708 51. Means JC, Passarelli AL. Viral fibroblast growth factor, matrix metalloproteases, and caspases
709 are associated with enhancing systemic infection by baculoviruses. Proceedings of the National
710 Academy of Sciences of the United States of America. 2010;107(21):9825-30.

711 52. Roques P, Gras G. Chikungunya fever: focus on peripheral markers of pathogenesis. The Journal
712 of infectious diseases. 2011;203(2):141-3.

713



bioRxiv preprint doi: <https://doi.org/10.1101/2021.05.26.445768>; this version posted May 26, 2021. The copyright holder for this preprint (which was not certified by peer review) is the author/funder, who has granted bioRxiv a license to display the preprint in perpetuity. It is made available under aCC-BY 4.0 International license.

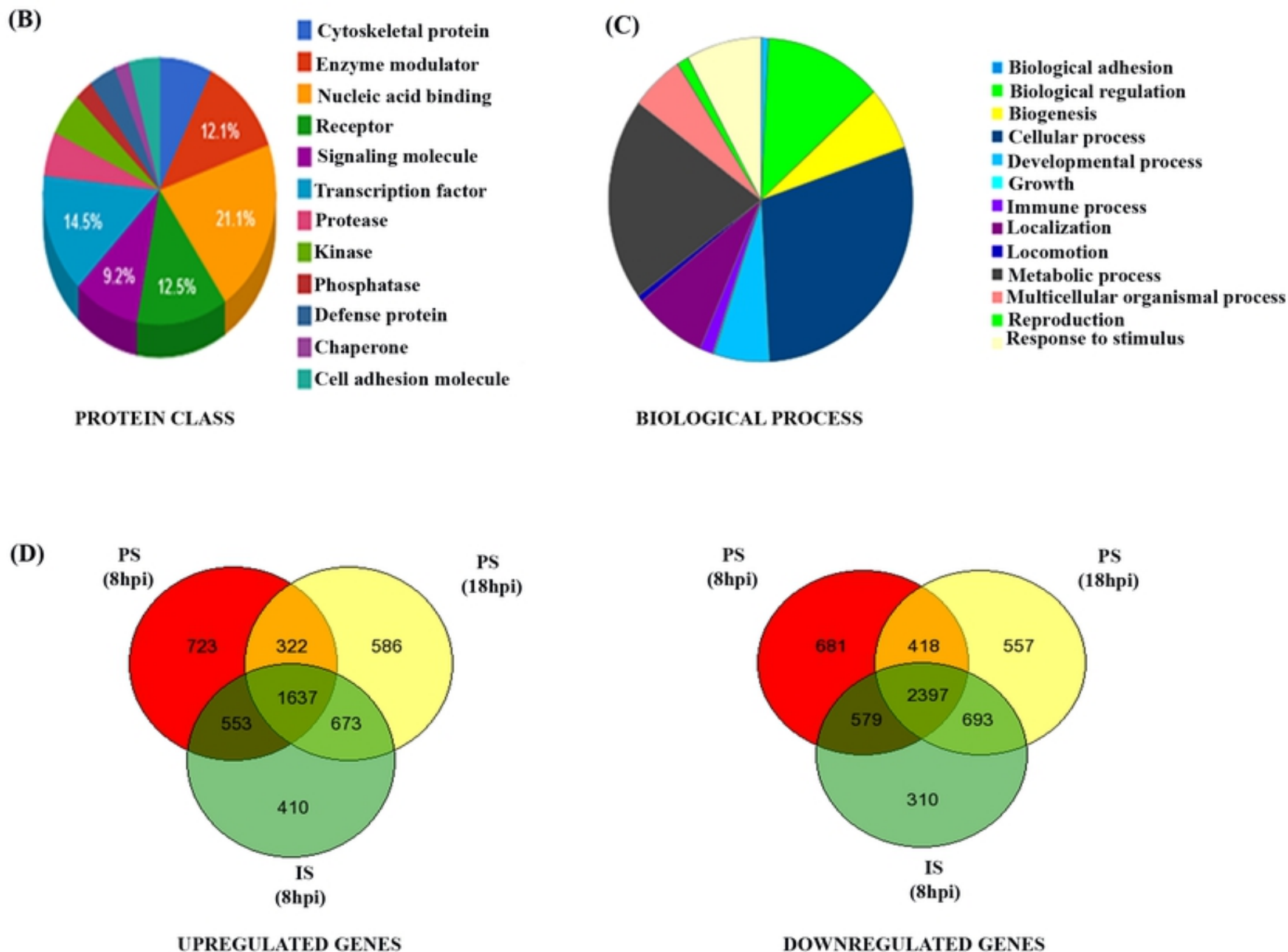
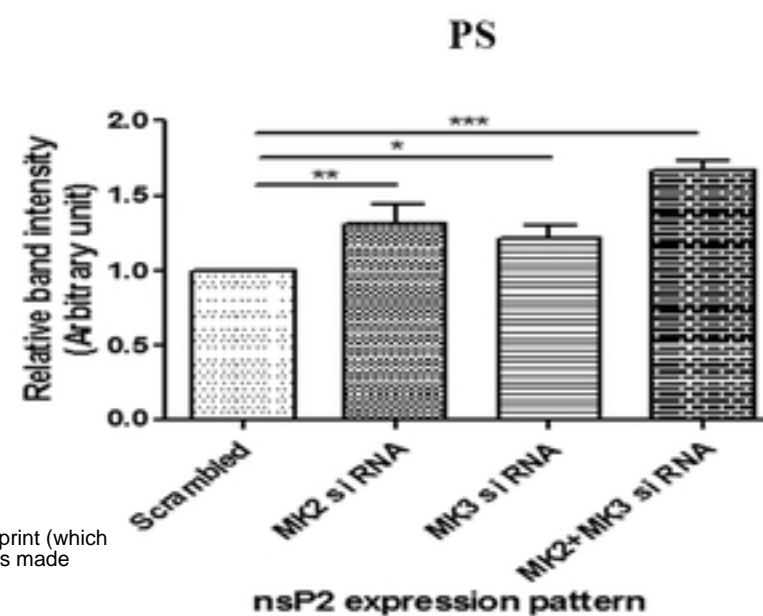
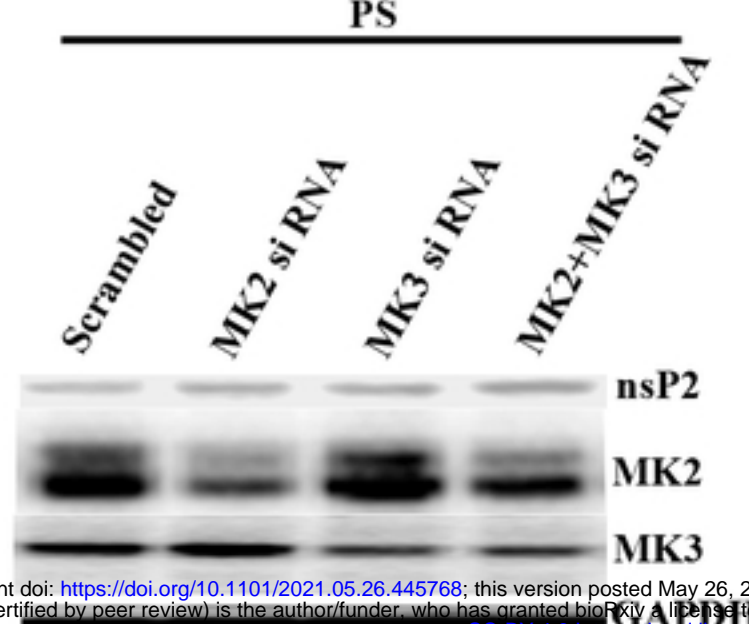


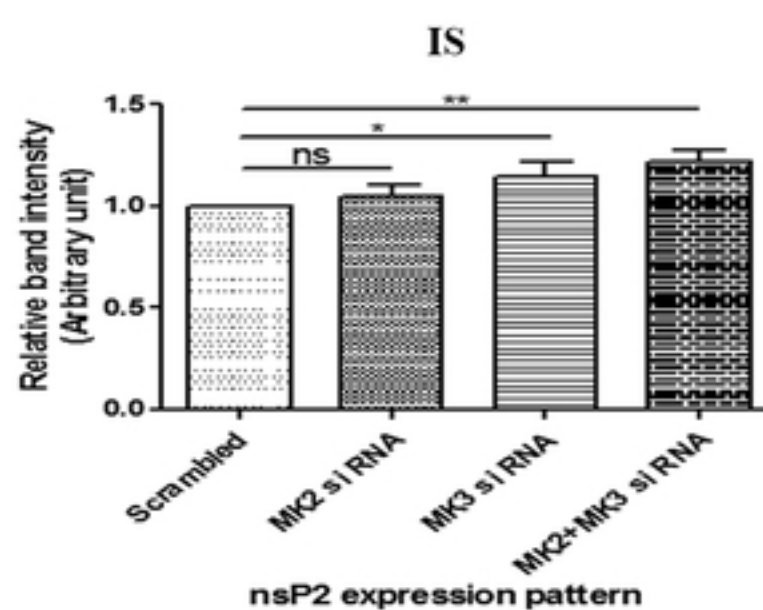
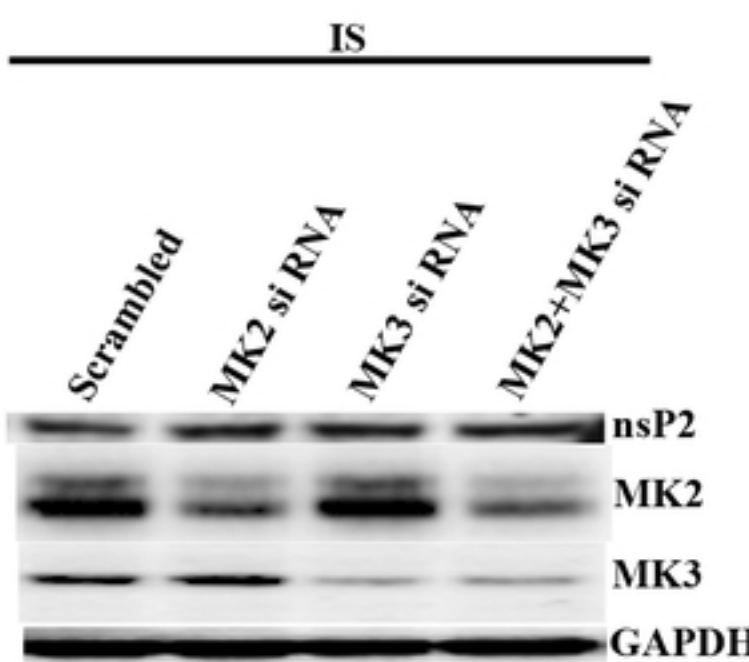
Fig 1

Figure 1

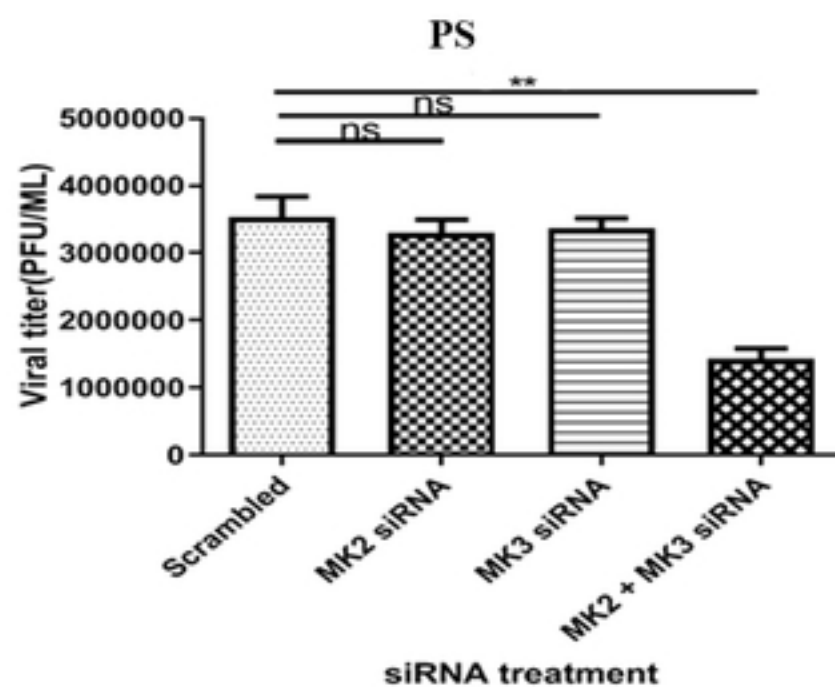
(A)



(B)



(C)



(D)

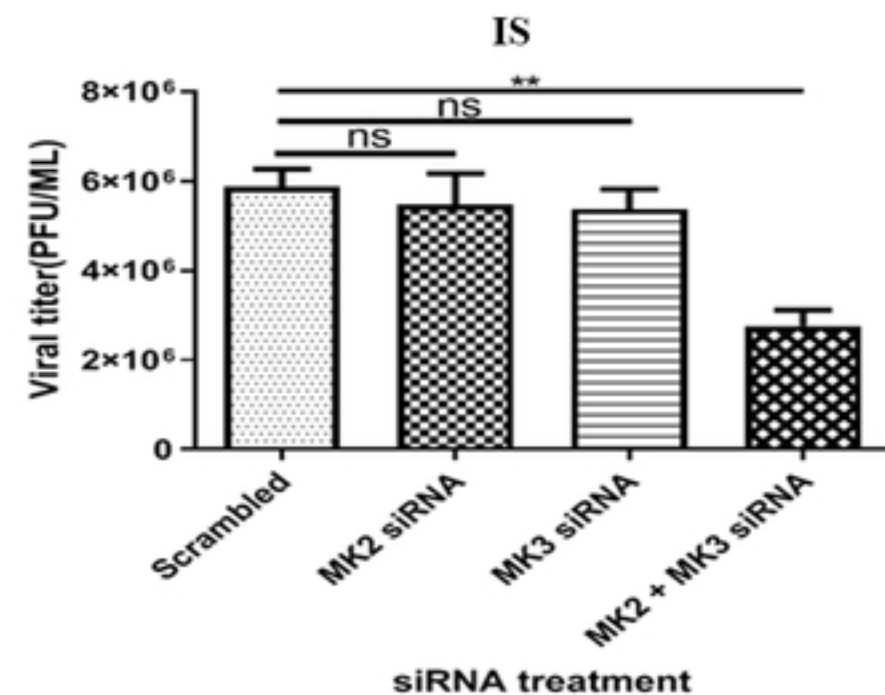


Fig 2

Figure 2

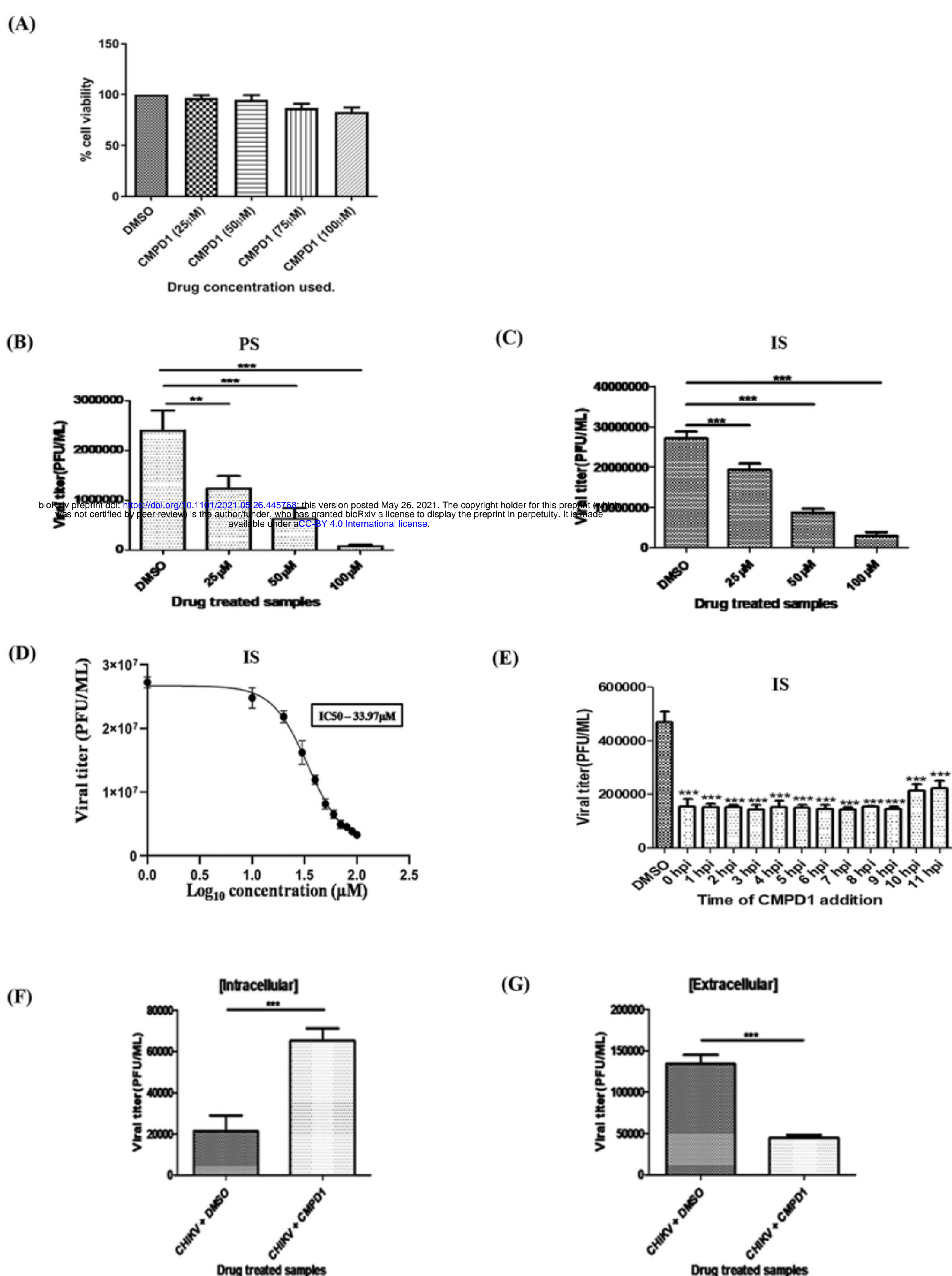
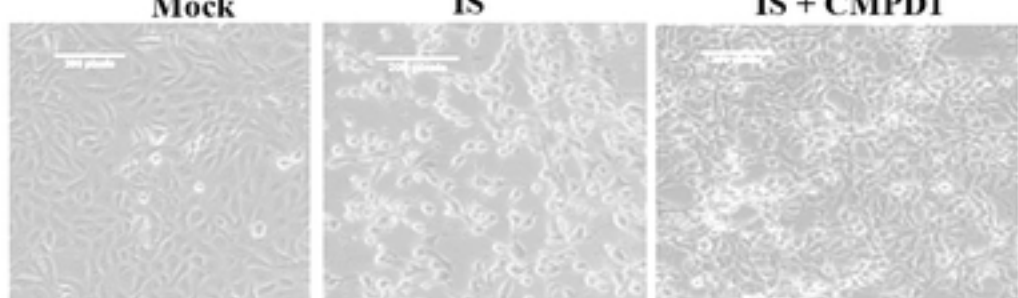
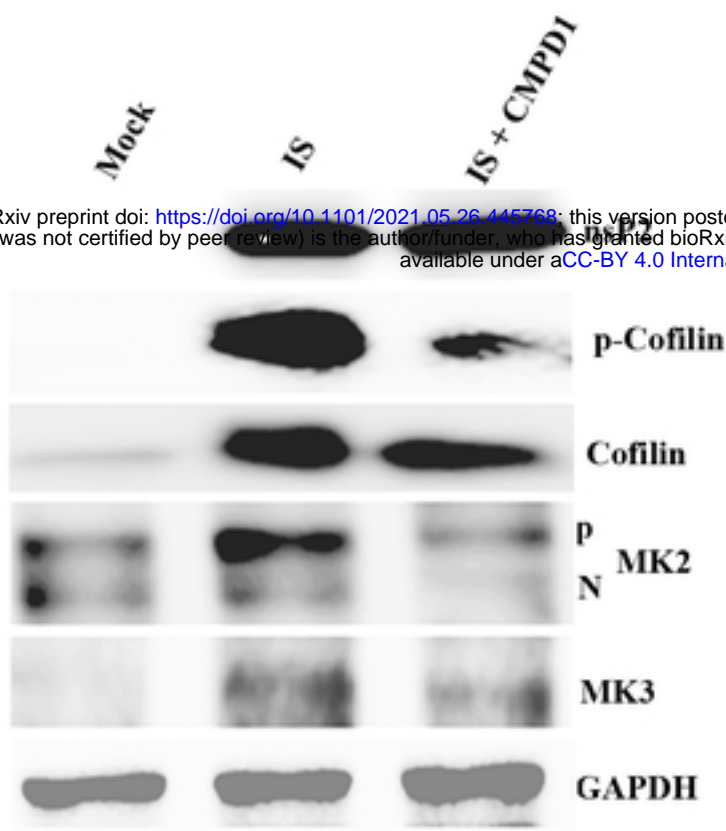
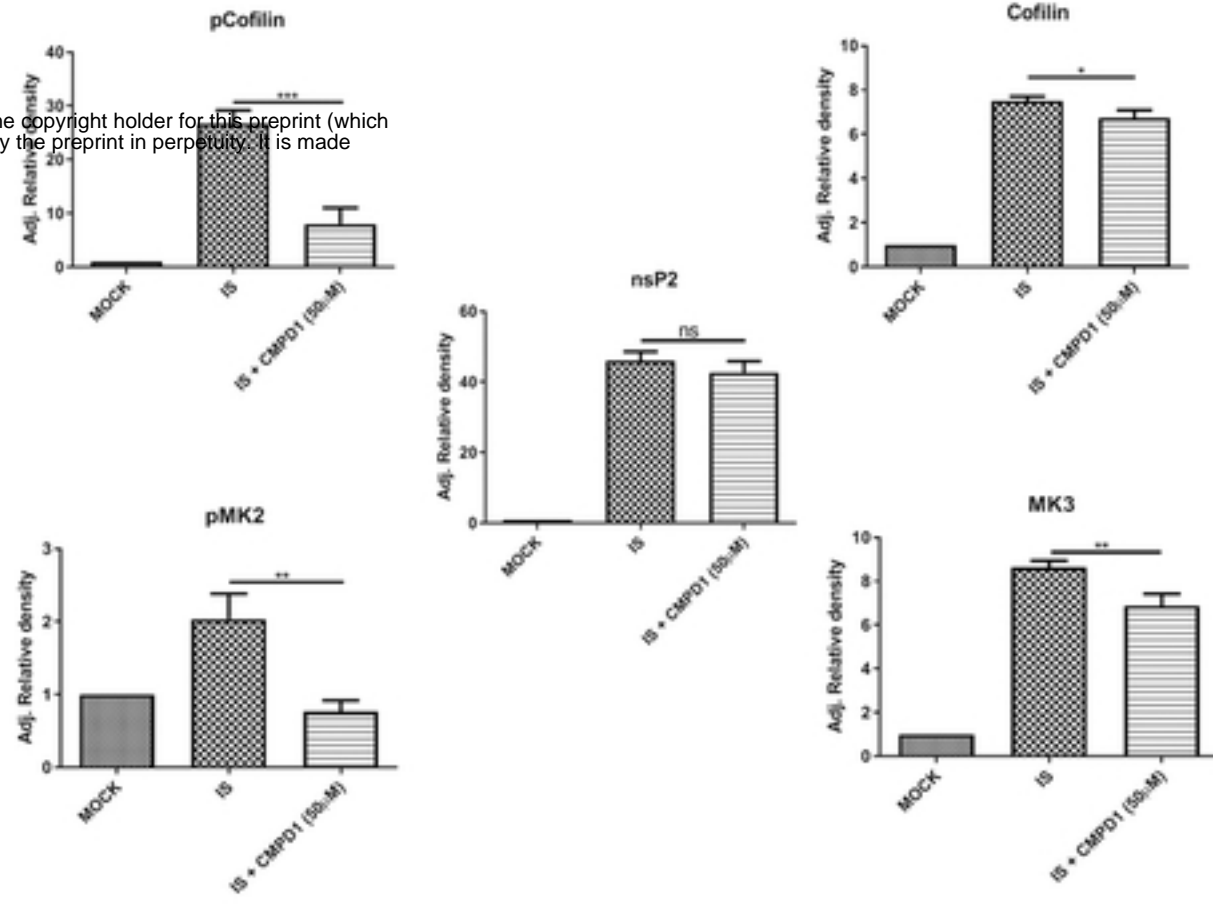
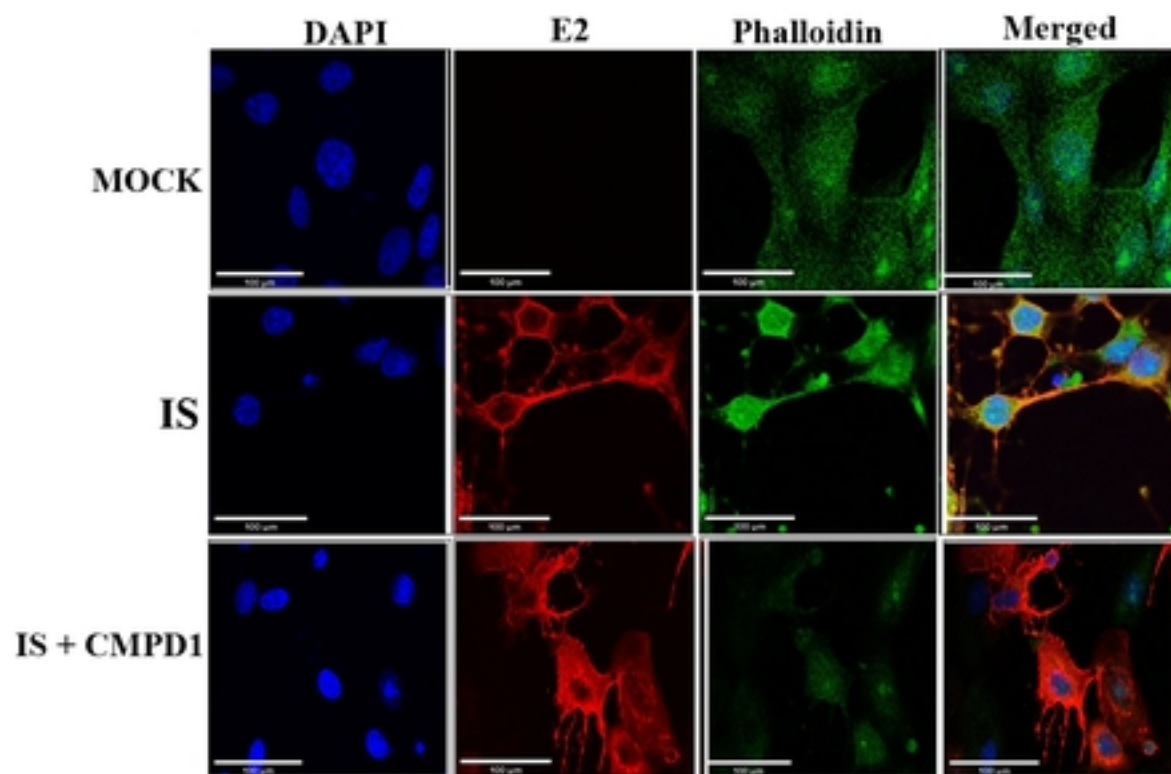
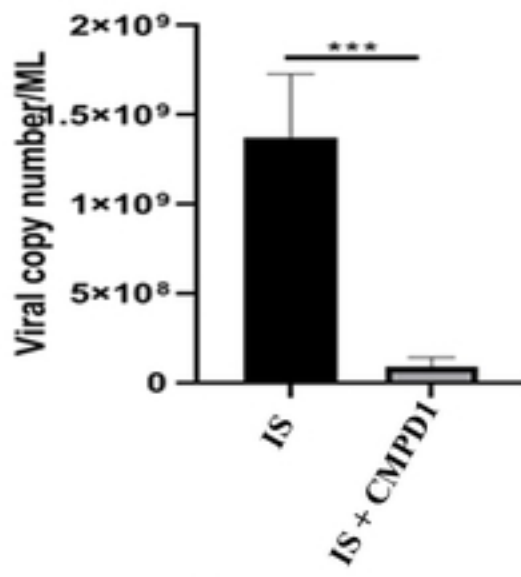


Fig 3

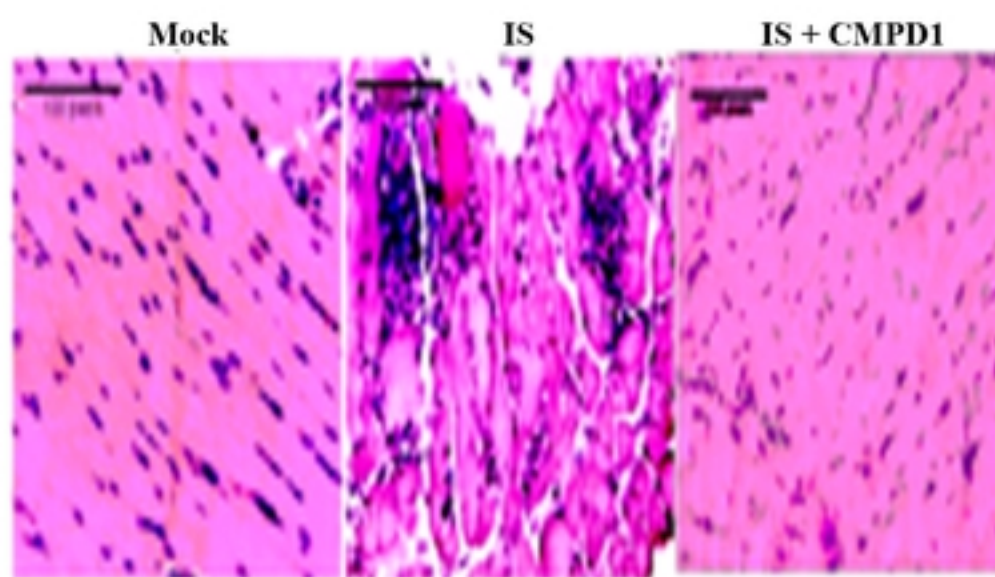
Figure 3

(A)**(B)****(C)****(D)****Fig 4****Figure 4**

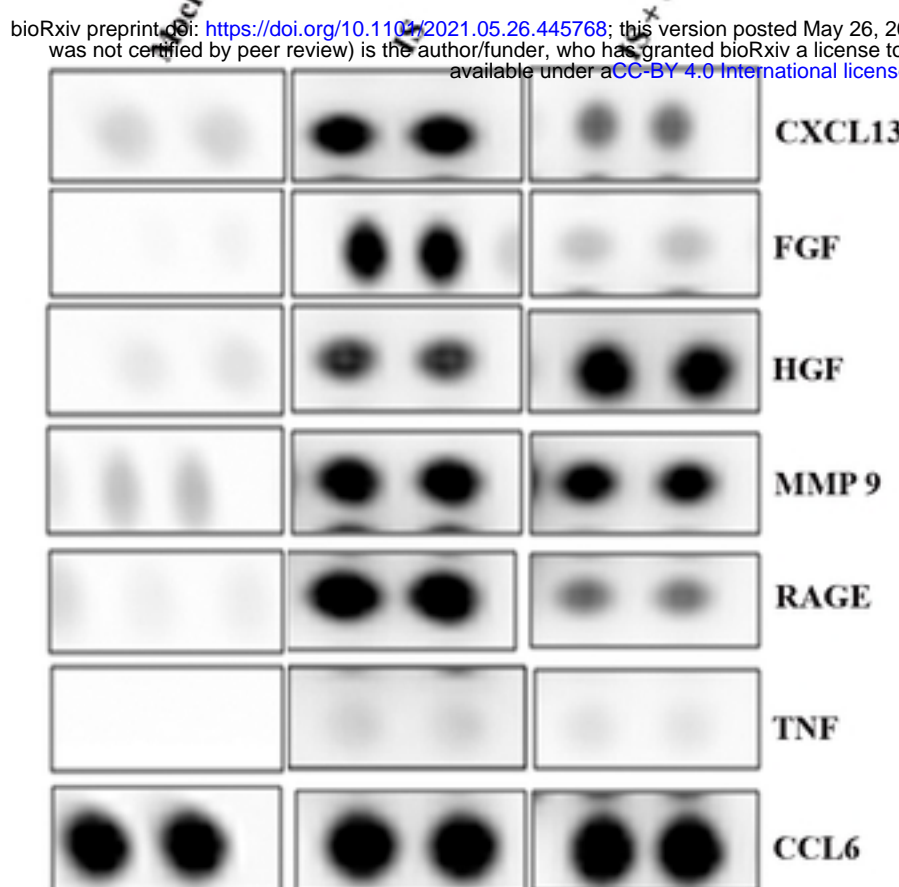
(A)



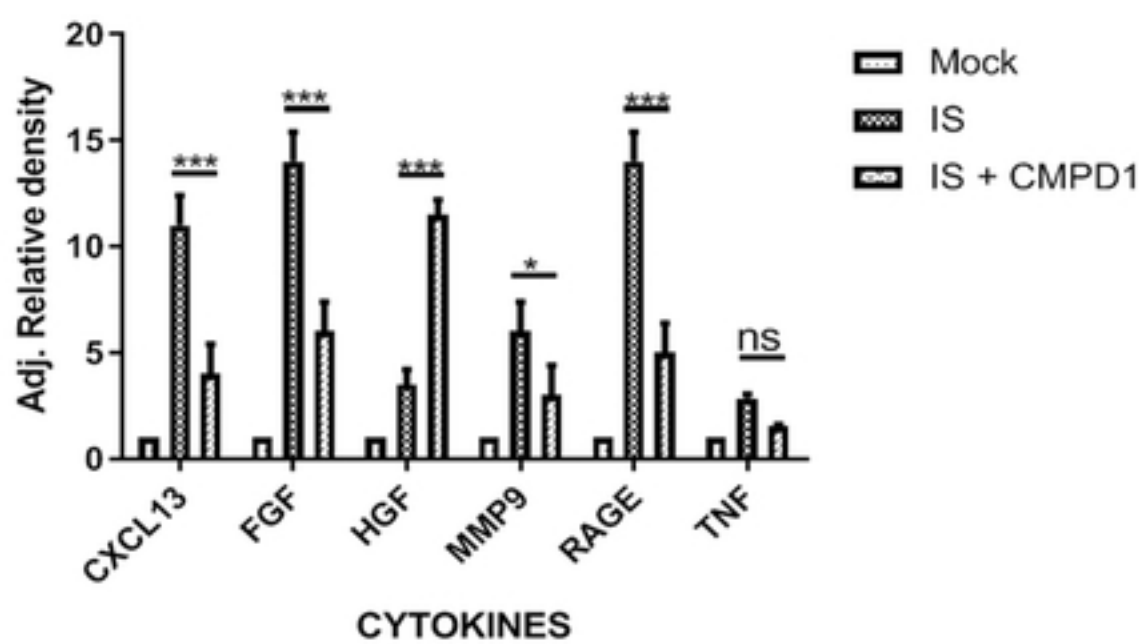
(B)



(C)



(D)



(E)

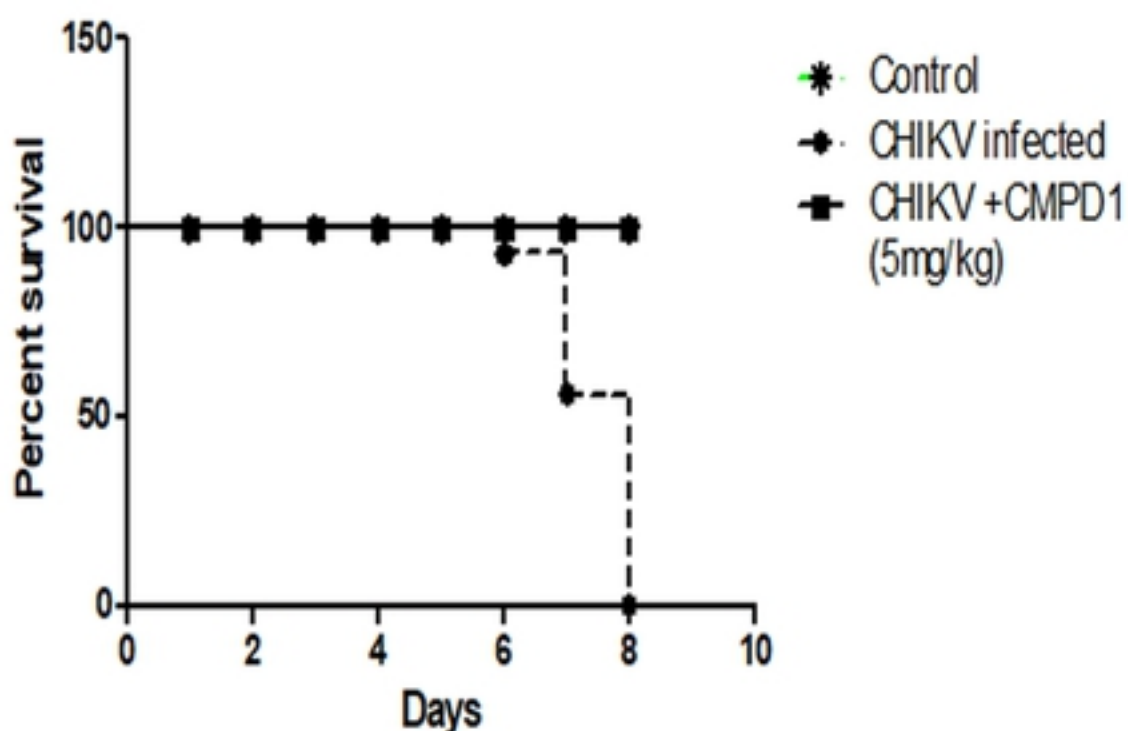
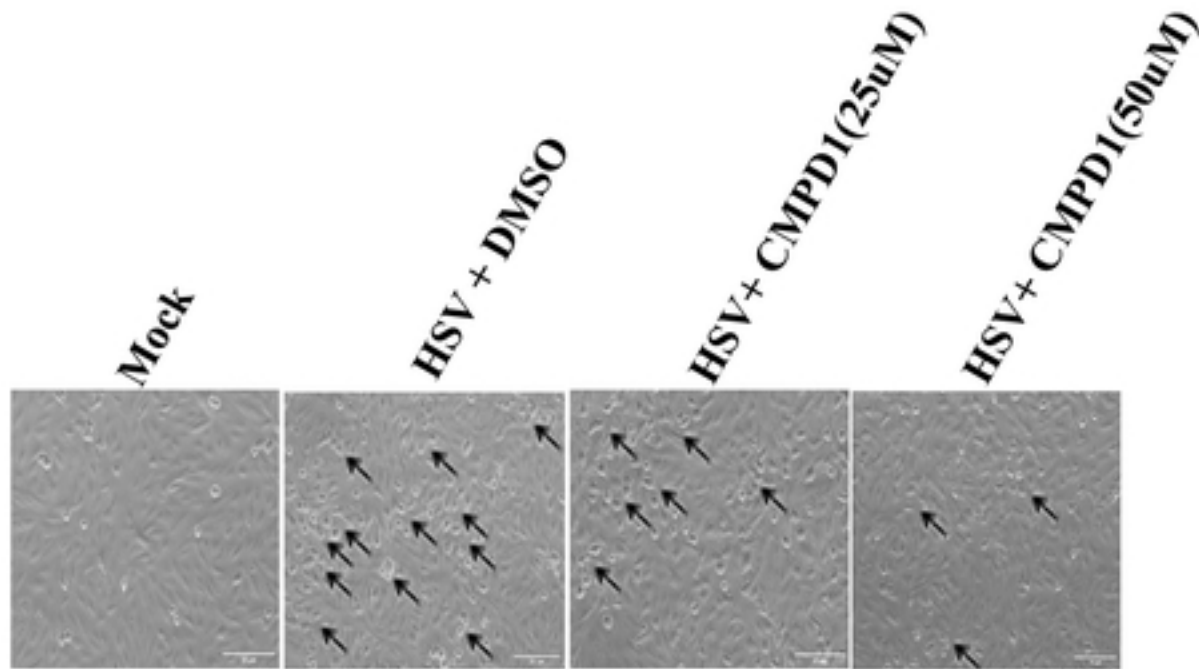


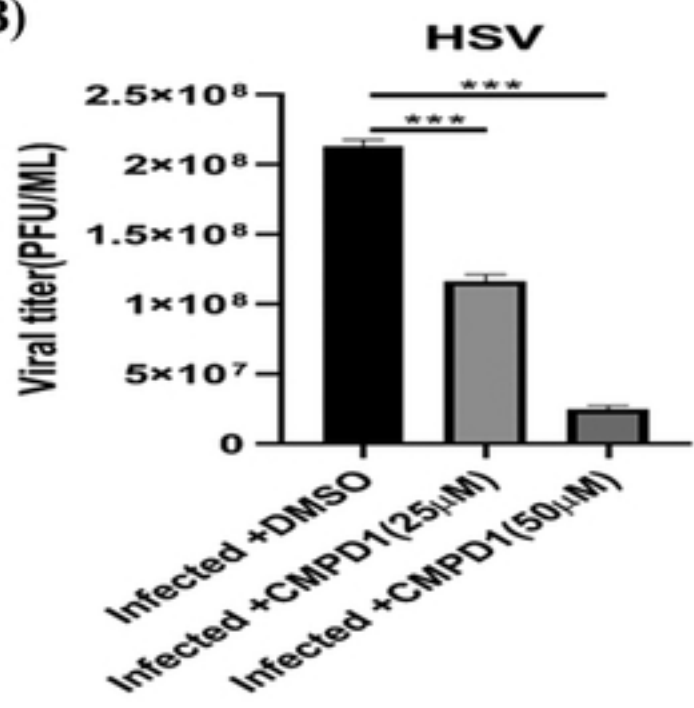
Fig 5

Figure 5

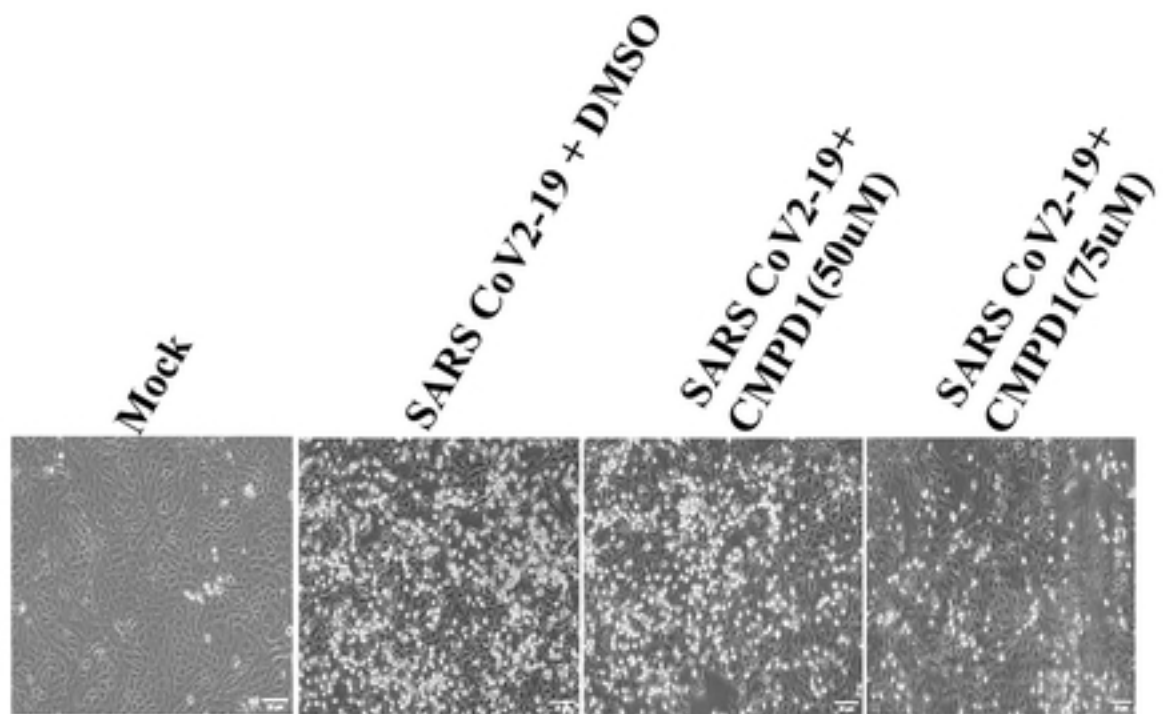
(A)



(B)



(c)



(d)

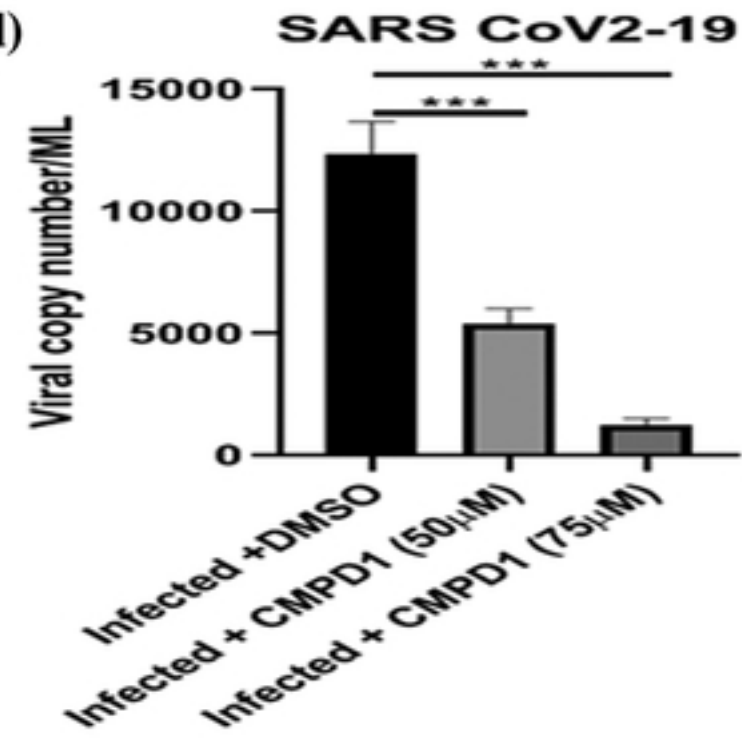
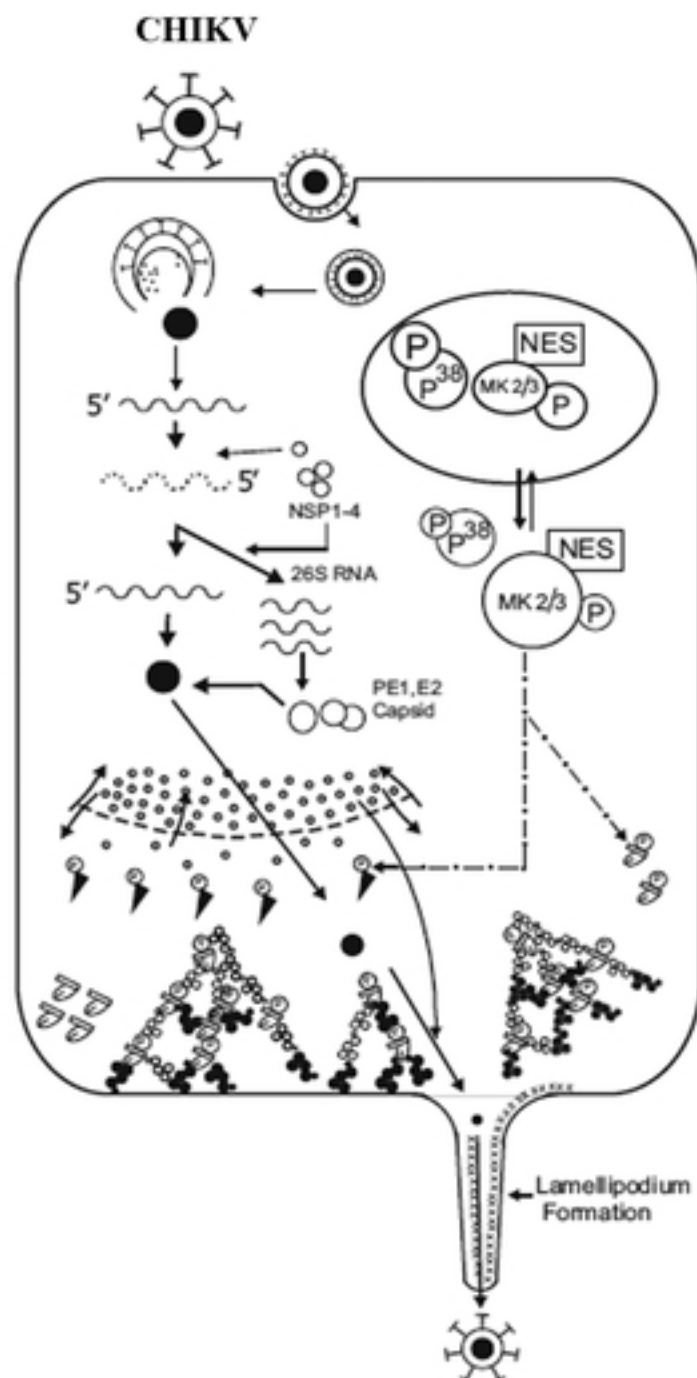


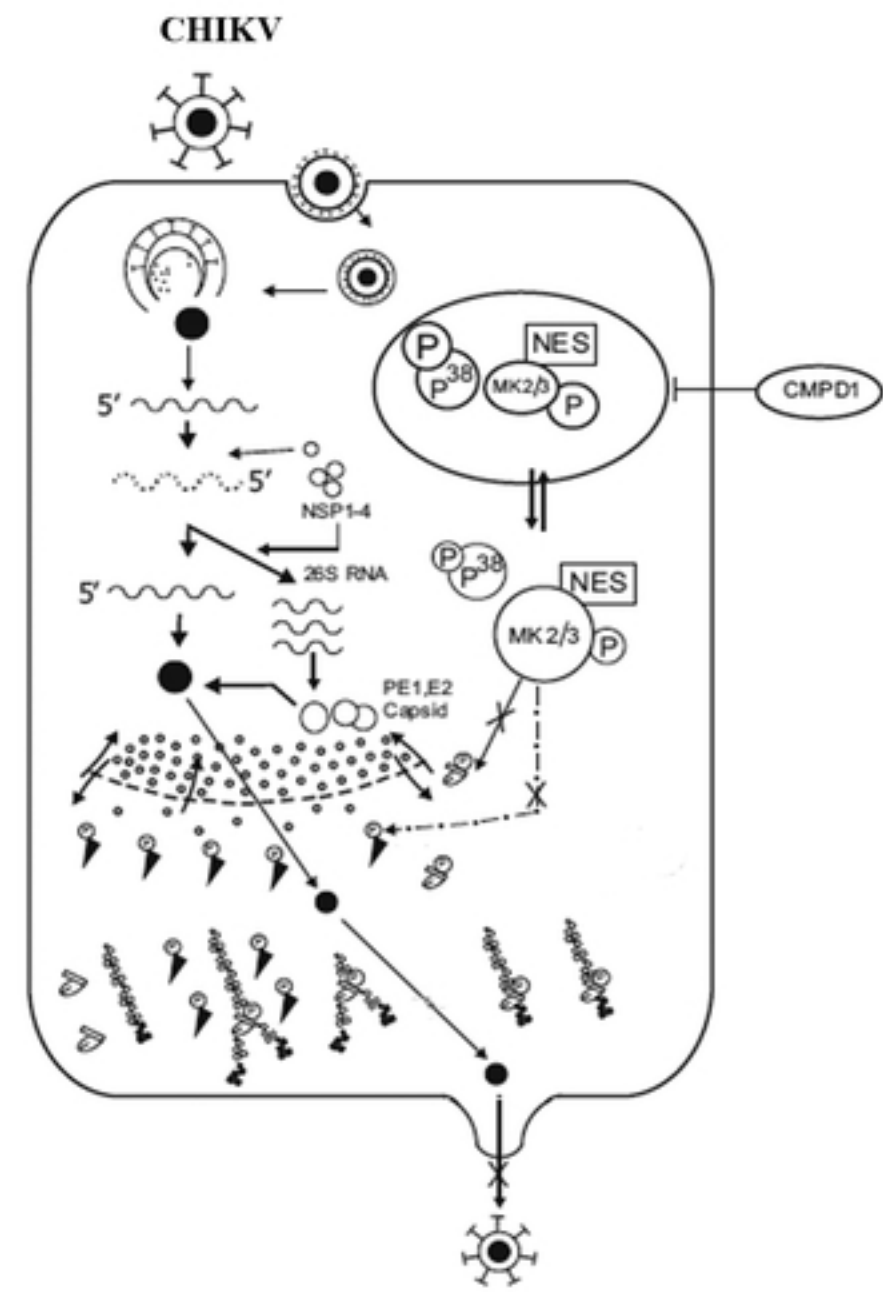
Figure 6

Figure 6

(A)



(B)



- ▲ ATP action
- ADP action
- ▶ Collin
- P-collin
- Arp 2/3
- Plasma membrane
- P. Arp 2/3

Fig 7**Figure 7**